7-2024

ABC Efflux Transporters and Solute Carriers in the Early Developing Brain of a Marsupial Monodelphis domestica (South American Gray Short-Tailed Opossum)

Yifan Huang

Katarzyna M. Dziegielewska

Mark D. Habgood

Fiona Qiu

Ana C. Leandro
The University of Texas Rio Grande Valley, ana.leandro@utrgv.edu

See next page for additional authors

Recommended Citation

Huang, Y., Dziegielewska, K. M., Habgood, M. D., Qiu, F., Leandro, A. C. C., Callaghan, P. D., Curran, J. E., VandeBerg, J. L., & Saunders, N. R. (2024). ABC Efflux Transporters and Solute Carriers in the Early Developing Brain of a Marsupial Monodelphis domestica (South American Gray Short-Tailed Opossum). The Journal of comparative neurology, 532(7), e25655. https://doi.org/10.1002/cne.25655

Journal of Comparative Neurology

WILEY

JCN RESEARCH IN SYSTEMS NEUROSCIENCE THE JOURNAL OF COMPARATIVE NEUROLOGY

RESEARCH ARTICLE OPEN ACCESS

ABC Efflux Transporters and Solute Carriers in the Early Developing Brain of a Marsupial *Monodelphis domestica* (South American Gray Short-Tailed Opossum)

Yifan Huang[1] | Katarzyna M. Dziegielewska[1] | Mark D. Habgood[1] | Fiona Qiu[1] | Ana C. C. Leandro[2] | Paul D. Callaghan[3] | Joanne E. Curran[2] | John L. VandeBerg[2] | Norman R. Saunders[1]

[1]Department of Neuroscience, Monash University, Melbourne, Victoria, Australia | [2]Division of Human Genetics and South Texas Diabetes and Obesity Institute, School of Medicine, The University of Texas Rio Grande Valley, Brownsville, Texas, USA | [3]ANSTO—Australia's Nuclear Science and Technology Organisation, Lucas Heights, New South Wales, Australia

Correspondence: Norman R. Saunders (norman.saunders@monash.edu)

Received: 14 December 2023 | **Revised:** 28 May 2024 | **Accepted:** 19 June 2024

Funding: Part of this research was conducted in facilities constructed at The University of Texas Rio Grande Valley (UTRGV) with support from NIH grant C06 RR020547, Funding provided by Katarzyna M Dziegielewska and Norman R Saunders.

Keywords: ABC efflux transporter | brain development | *Monodelphis domestica* | paracetamol | placenta | rat | RRID:NCBITaxon_13616 | RRID:SCR_002344 | RRID:SCR_006281 | SLC transporter

ABSTRACT

This study used a marsupial *Monodelphis domestica*, which is born very immature and most of its development is postnatal without placental protection. RNA-sequencing (RNA-Seq) was used to identify the expression of influx and efflux transporters (ATP-binding cassettes [ABCs] and solute carriers [SLCs]) and metabolizing enzymes in brains of newborn to juvenile *Monodelphis*. Results were compared to published data in the developing eutherian rat. To test the functionality of these transporters at similar ages, the entry of paracetamol (acetaminophen) into the brain and cerebrospinal fluid (CSF) was measured using liquid scintillation counting following a single administration of the drug along with its radiolabelled tracer [^{3}H]. Drug permeability studies found that in *Monodelphis*, brain entry of paracetamol was already restricted at P5; it decreased further in the first week of life and then remained stable until the oldest age group tested (P110). Transcriptomic analysis of *Monodelphis* brain showed that expression of transporters and their metabolizing enzymes in early postnatal (P) pups (P0, P5, and P8) was relatively similar, but by P109, many more transcripts were identified. When transcriptomes of newborn *Monodelphis* brain and E19 rat brain and placenta were compared, several transporters present in the rat placenta were also found in the newborn *Monodelphis* brain. These were absent from E19 rat brain but were present in the adult rat brain. These data indicate that despite its extreme immaturity, the newborn *Monodelphis* brain may compensate for the lack of placental protection during early brain development by upregulating protective mechanisms, which in eutherian animals are instead present in the placenta.

1 | Introduction

Extant mammals are categorized into three major lineages: egg-laying monotremes (Prototheria), marsupials (Metatheria), and eutherian mammals (Eutheria). Marsupials have been used as a powerful comparative model to understand mammalian biology. Since their evolutionary separation, metatherians and eutherians have developed some distinctive anatomic, physiologic, and genetic features, most notably in embryogenesis (Frankenberg et al. 2016). In eutherian mammals such as the human and

rodent, the placenta acts as an interface that controls the entry of essential nutrients (Zhang et al. 2015) and provides some protection against the entry of potentially harmful agents such as environmental toxins or drugs ingested by or administered to the mother (Saunders et al. 2019). In contrast, marsupials have a rudimentary placenta that is present for only a few days before birth (Tyndale-Biscoe 2005). Additionally, marsupials are born at an extremely early stage of development, particularly of their central nervous system (CNS), compared to eutherians. Thus, *Monodelphis domestica* (gray short-tailed opossum) at birth has a stage of brain development similar to that of a 5–6-week postconception human fetus or embryonic day (E)13 rat (Saunders et al. 1989; Workman et al. 2013).

The adult brain of mammals is protected by a number of mechanisms present in the cellular interfaces between the circulating blood and the brain and cerebrospinal fluid (CSF); these interfaces also tightly control the entry of ions and metabolically important molecules as well as regulating the exit of metabolites (Davson and Segal 1996; Saunders et al. 2018). In addition to passive diffusion, brain entry of lipid soluble molecules, including many drugs, is affected by their interactions with efflux/influx mechanisms. The main family of efflux transporters is the ATP-binding cassette (ABC) superfamily of transmembrane channel proteins that use active transport with energy derived from the conversion of ATP to ADP to move substrates across lipid cell membranes (Linton 2007). A characteristic of these transporters is the presence of at least four domains: two transmembrane domains (TMDs) and two nucleotide-binding domains (NBDs). The TMDs embedded in the lipid bilayer recognize, bind, and translocate substrates, whereas NBDs are located in the cytoplasm and bind and hydrolyze ATP (Linton 2007; Rees, Johnson, and Lewinson 2009; Vasiliou, Vasiliou, and Nebert 2009). These consist of seven subfamilies from ABC (A–G) sorted by genetic sequence similarity and TMDs. A total of 49 genes are present in humans with varying transport functions, including lipid, steroid, and drug transport (Rees, Johnson, and Lewinson 2009). Several of these transporters have also been implicated in the exclusion of drugs.

Another transporter superfamily, solute carriers (SLCs), currently consists of 458 cell membrane transporters distributed across 66 families (Povey et al. 2001; Hediger et al. 2013). Although SLCs have been less extensively studied compared to ABC transporters, they have a wide variety of functions, including ion, amino acid, sugar, and drug transport, and are gradually being recognized as therapeutic drug targets for a wide range of diseases (Rask-Andersen et al. 2013). However, rather than requiring active transport like the ABC transporters, SLCs utilize facilitated or secondary active transport to move molecules across cell membranes (Stein and Litman 2014).

Most research into drug resistance has so far been focused on the upregulation of ABC efflux transporters to restrict drug entry across barrier interfaces (e.g., Löscher 2007; Housman et al. 2014), but other explanations such as drug inactivation due to metabolizing enzyme modulation have also been explored (Ghosh et al. 2011). Although not a physical barrier in the same sense as the blood–brain and placental barriers, metabolizing enzymes play an important role in the breakdown of drugs and subsequent transport and therefore have been dubbed the metabolic barrier (Strazielle and Ghersi-Egea 1999). Metabolic enzymes are predominantly expressed in the liver but also occur in many other regions, including within brain endothelial cells (Ghosh et al. 2010), choroid plexus (Dey, Jones, and Nebert 1999), and placenta (Ejiri et al. 2001). ABC transporters and SLCs appear to be highly conserved among species; however, their affinities to specific drugs vary (Dean and Dean 2002; Ferrada and Superti-Furga 2022). In addition, although the majority of metabolizing enzymes appear to function similarly across species, there appear to be some species variations in drug-metabolizing enzymes, particularly in relation to gene expression and activity of cytochrome p450 enzymes (Gonzalez and Nebert 1990; Gonzalez 1998).

The functional status of these mechanisms in embryonic and early postnatal brain has been a subject of much debate over several decades, but there is increasing evidence that many of these mechanisms are functionally effective from early in brain development, with some important differences from the adult (Saunders et al. 2018, 2019, 2023). The role of the placenta in limiting fetal brain entry of maternally administered drugs has also been extensively studied (for review, see Syme, Paxton, and Keelan 2004; Mao and Chen 2022). Given the transient nature of the placenta in marsupials and their very early stage of brain development at birth, it is of particular biological interest to know how well these mechanisms are developed in marsupial fetal brain compared to the brains of eutherian fetuses that have the added nutritional and protective functions of a placenta.

We have studied this problem in *Monodelphis* (Figure 1) at different postnatal ages using a combination of RNA-sequencing (RNA-Seq) of brain cortex and assessing the functionality of such mechanisms in response to the administration of a commonly used clinical drug, paracetamol. Our transcriptomic analysis concentrated on the expression of efflux and influx transporters and their associated metabolizing enzymes. Results obtained from these experiments were then compared to published data on the transcriptome of the developing rat brain and the available transcriptome of the late gestation rat placenta (Koehn et al. 2021). The choice of paracetamol as a test drug was based on two main criteria: (i) Paracetamol, a widely used analgesic/antipyretic, is one of the first drugs advised for use in neonate human babies (World Health Organization 2012; Australian Medicines Handbook 2022); therefore, it is relevant for the comparison with a eutherian fetal/newborn rat made in the present study. (ii) The actual mechanisms controlling paracetamol transfer into the brain are not known and have been suggested to involve several transporters (e.g., Zamek-Gliszczynski et al. 2005, 2006; Blazquez et al. 2014; Koehn et al. 2019, 2021), allowing us to obtain some information on the overall functionality of these transporters in the developing marsupial brain.

Results showed that some of efflux and influx mechanisms that are present in the rat placenta but not in its fetal brain are already present in the newborn marsupial brain, indicating the importance of the placenta in eutherians. This also highlights some evolutionary adaptations in the brain-protective mechanisms in a marsupial that mostly develop in the absence of placental protection.

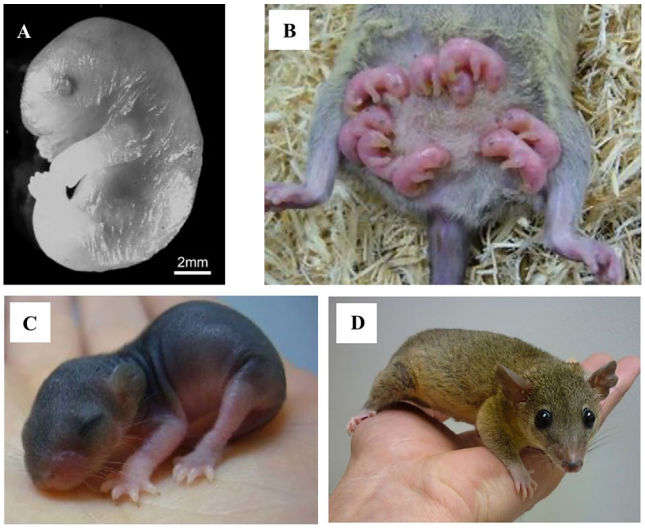

FIGURE 1 | The gray short-tailed opossum (*Monodelphis domestica*) at four developmental ages: (A) postnatal day (P)0, (B) P7 attached to the mother, (C) P28, and (D) fully grown adult female. *Monodelphis* are born very immature and at an embryonic stage of brain development compared to eutherian mammals. The gestational period lasts only 14 days, with a transient placenta present for only the final days before birth. The brain development of newborn *Monodelphis* is roughly equivalent to that of the embryonic day (E) 13 rat (Saunders et al. 1989; Workman et al. 2013). As an extremely immature newborn, the skin and craniofacial features of *Monodelphis* are noticeably tougher compared to their eutherian counterparts at a similar developmental stage (Smith 2001). In addition, the development of some organs such as the heart and lungs are also more advanced in *Monodelphis*. As a consequence, they are able to survive early birth (Cardoso-Moreira et al. 2019). *Source*: (B)–(D) From Wheaton et al. (2011).

2 | Materials and Methods

M. domestica (RRID: NCBITaxon_13616), South American gray short-tailed opossums, were supplied from two breeding colonies, one maintained by the University of Melbourne Biological Research Facility and the other at The University of Texas Rio Grande Valley (UTRGV). The use of animals in Melbourne was approved by the University of Melbourne Ethics Committee (Ethics Approval AEC: 10270) and conducted in compliance with the Australian National Health and Research Guidelines. The use of animals in Texas was approved by the UTRGV IACUC (Protocol AUP-22-07). Animal husbandry was the same in both facilities and followed conditions described previously (Saunders et al. 1989; VandeBerg and Williams-Blangero 2010; Wheaton et al. 2013). Briefly, animals were housed in polycarbonate boxes in temperature- and humidity-controlled (27°C; 60% humidity) rooms with a 14:10 h light/dark cycle with food and water given ad libitum.

Age groups used for the RNA-Seq analysis study were neonates (P0–P5), early postnatal pups (P8), and juveniles (P109). Age groups used for the drug transfer studies were: neonates (P0 and P5), early postnatal pups (P8), late postnatal pups (P28), pups at or close to weaning (P62), and juveniles (P109–P113). P0 was the day of birth. For blinding in drug transfer studies, animals were randomly allocated to each treatment group by the Animal House staff, who were not aware of the type of experiment performed.

2.1 | RNA-Seq Experiments and Analysis

Animals at P0, P5, P8, and P109 were terminally anesthetized with inhaled isoflurane (IsoFlo 100% w/w, Abbott Laboratories, Chicago, IL, United States) and then segments of brain cortex were dissected out in RNase-free conditions. Brain samples contained the whole thickness of the cortex wall, as described previously for the rat (Koehn et al. 2021 and 2020). From P8 to P109, an equal number of males and females were used, but at P0 and P5, it was not possible to determine the sex of the pups; therefore, these were mixed samples. RNeasy Plus Mini Kit (QIAGEN, Hilden, Germany) was used to extract RNA from P109 brain samples, whereas RNeasy Plus Micro Kit (QIAGEN) was used for P0, P5, and P8 animals according to manufacturer's specifications.

For samples sequenced in Melbourne, RNA was delivered on dry ice to the Australian Genome Research Facility (AGRF) for Illumina and next-generation sequencing for quality control and analysis. Runs were 100 bp single reads, and raw FASTAq data were obtained.

For samples sequenced in Texas, total RNA concentration was estimated using a PicoGreen method (Qubit RNA BR kit, Invitrogen, USA) according to the manufacturer instructions (Thermo Fisher Scientific, Waltham, MA, USA). RNA quality was also estimated using a Qubit RNA Integrity and Quality (IQ) assay (Invitrogen) and an RNA Screen tape on the Agilent 4200 TapeStation (RRID:SCR_018435) according to the manufacturer instructions (Agilent Technologies, Santa Clara, CA, USA). Samples with an RNA integrity number superior to or equal to 7 passed the quality control. RNA samples were processed for Stranded mRNA Sequence with polyA selection (Illumina Stranded mRNA prep, Illumina, USA) and sequenced on Illumina NovaSeq 6000 (RRID:SCR_016387) output mode with a sequencing configuration of 2×51 paired-end reads. Runs were 100 bp single reads, and raw FASTAq data were obtained.

2.1.1 | Dataset Analysis

Data obtained from both sequencing facilities were processed using the Galaxy Australia platform (RRID:SCR_006281) and their online software packages (Jalili et al. 2020). Default parameters were used unless otherwise specified. Data were checked for quality using FastQC (RRID:SCR_014583, Galaxy version 0.72) and aligned with HISAT2 (RRID:SCR_015530, Galaxy version 2.1.0) using the monDom5 (*M. domestica*) reference genome and annotation file from the Ensembl database (RRID:SCR_002344, ASM229v1). Count files were then generated using featureCounts (RRID:SCR_012919, Galaxy version 1.6.4+galaxy1). Gene differential expression analysis was received using three pathways: EdgeR (likelihood ratio; RRID:SCR_012802, Galaxy version 3.24.1+galaxy1), DESeq2 (RRID:SCR_012802, Galaxy version 2.11.40.6+galaxy1), and limma-voom (RRID:SCR_010943, Galaxy version 3.38.3+galaxy3). Unannotated genes were mapped using a combination of BioMart (RRID:SCR_019214, Kinsella et al. 2011), bioDBnet (Mudunuri et al. 2009), and String (RRID:SCR_005223,

TABLE 1 | List of drugs used, their abbreviation, dose, supplier, and catalog number.

Drug	Abbreviation	Dose	Supplier	Catalog #
[^{3}H]-Paracetamol	[^{3}H] PARA	Trace	American Radiolabeled Chemicals	ART 0679
Paracetamol	PARA	15 mg/kg	Sigma Aldrich	A7085-100G

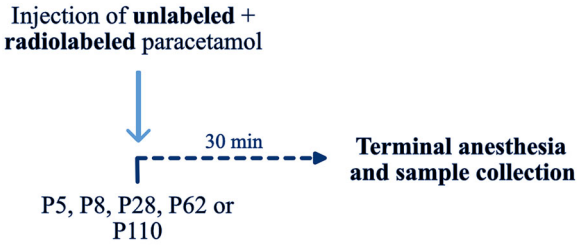

FIGURE 2 | Injection schedule for acute single-drug experiments in *Monodelphis*. Animals at five age groups, P5, P8, P28, P62, or P110, were administered a single dose of either paracetamol (PARA, 15 mg/kg) via *i.p.* injection along with its respective radiolabelled tracer, [^{3}H]-paracetamol. Animals were terminally anesthetized, and blood, brain, and CSF samples were collected 30 min following injection for liquid scintillation counting. CSF, cerebrospinal fluid.

Szklarczyk et al. 2019) with a number of genes remaining unidentified. The complete list of identified transcripts (counts per million, CPM) is available in Table S1.

2.1.2 | Statistical Analysis

Expression levels were considered statistically different if present in at least two of the three analysis pathways at a statistical threshold of an adjusted p value <0.05 (EdgeR, FDR; DESeq2, p-adj; limma-voom, adj.P.Val) and counts are ≥1 CPM in at least one comparison group as described previously for *Monodelphis* (Wheaton et al. 2020) and rat (Koehn et al. 2021) transcriptomes.

2.2 | Drug Entry Experiments

Entry of paracetamol into the brain and CSF of the *Monodelphis* at P5, P8, P28, P62, and P110/113 (combined as P110) was measured using liquid scintillation counting as described previously (Koehn et al. 2019). A drug dose of 15 mg/kg (Table 1) was selected based on its use in clinical practice (Australian Medicines Handbook 2022) and in a previous rat study (Koehn et al. 2019). Paracetamol was dissolved in sterile 0.9% sodium chloride solution, and injected volumes were adjusted for the body weight of the animal.

Blood (right cardiac ventricle), brain (cortex), and CSF (cisterna magna) samples were collected 30 min following intraperitoneal (*i.p.*) administration of paracetamol (15 mg/kg) along with its radiolabelled tracer, [^{3}H]-paracetamol (Table 1), using the same protocol as Koehn et al. (2019). Injection protocol is illustrated in Figure 2. At P5, blood and CSF samples were pooled in groups of 2–3 to ensure sufficient counts for liquid scintillation counting. P5 values reported in this study are therefore an average of multiple pools. At older ages, pooling was not required.

Samples were processed immediately after collection. Blood was centrifuged at 2000 × g for 5 min, and plasma supernatant was collected for analysis. CSF samples were examined for blood contamination and discarded if red blood cells were visible microscopically (Habgood et al. 1992). Brain samples were solubilized using 0.5 mL Soluene350 (PerkinElmer, Shelton, CT, USA) and incubated overnight at 36°C. All samples were weighed, transferred into scintillation vials, and 5 mL of scintillant (Emulsifier-safe, PerkinElmer) was added. Blank vials containing the same tissues without radioactivity and radioactive samples were counted on a liquid scintillation counter (Tri-Carb 4910 TR, PerkinElmer), and counts in disintegrations per minute (DPM) over 5 min were obtained. Background values from the blank vials were subtracted from each corresponding radioactive sample, and brain or CSF transfer was then calculated using the following equation:

$$\text{Brain or CSF transfer} = \frac{\text{Brain or CSF DPM (mg or } \mu\text{L)}}{\text{plasma DPM } (\mu\text{L})} \times 100\%$$

2.2.1 | Statistical Analysis

Statistical analysis for drug entry studies was conducted using GraphPad Prism (RRID:SCR_002798). Values were expressed as mean ± SD, and significance threshold was set at $p < 0.05$. An unpaired t-test was used for comparisons between two groups when appropriate; one-way ANOVA with Tukey's multiple comparisons test was used for comparisons between more than two groups.

2.2.2 | Autoradiography

Brains from paracetamol-treated *M. domestica* at P8 (injected with 0.33 μCi [^{3}H]-paracetamol) and at P100 (injected with 5 μCi [^{3}H]-paracetamol), as well as untreated un-injected controls at the same ages, were collected immediately following exsanguination (see above) and snap frozen by floating on aluminum foil in liquid nitrogen. Once frozen, samples were transferred to a −80°C freezer for storage until sectioning. Frozen brains were warmed to −20°C before using Leica CM3050 S cryostat (RRID:SCR_020214) to cut 20 μm sagittal sections that were placed on glass slides to dry.

Slides were developed as described previously (Koehn et al. 2021). Briefly, once dry, slides were exposed to ^{3}H-sensitive Carestream Biomax MR film (Sigma-Aldrich, St. Louis, MO, USA) and developed for 9 months together with control brains, which did not contain radiolabel. Standards (0.07–6.5 nCi/mg tissue and 1–35 nCi/mg tissue; Amersham Autoradiographic [^{3}H] microscales RPA506, batch 20) were included on each film. The films were scanned, and all images were manipulated to the same degree

to obtain an outline of control sections where there was enough contrast.

3 | Results

3.1 | Expression of ABC Efflux Transporters, Their Metabolizing Enzymes, and SLC

In order to investigate the developmental changes in the expression of ABC efflux transporters, their metabolizing enzymes, and SLCs in the *Monodelphis* brain, transcriptomic datasets were obtained at postnatal days P0, P5, P8, and P109 (juvenile), and analysis was conducted as described in Section 2.

A total of 34,985 transcripts were detected in the *Monodelphis* at the 4 ages analyzed, but of these, only 15,154 were present with an expression of >1 CPM (Table S1). ABC transporters expressed in the adult brain are described first, followed by a specific description of transporters that were differentially expressed at younger ages.

3.1.1 | ABC Efflux Transporters

Thirty-five ABC transporters from seven subfamilies—eight ABCAs, six ABCBs, eight ABCCs, four ABCDs, one ABCE, four ABCFs, and five ABCGs—were present in the *Monodelphis* brain at P0, P5, P8, and P109. These transporters are displayed in Figure 3 and Table S2.

3.1.1.1 | Adult (P109). In P109 animals, 33 ABC transporters were expressed at >1 CPM (Figure 3, Table S2), including 2 lipid transporters that were expressed at more than 200 CPM: *Abca2* (540 ± 22 CPM) and *Abca3* (224 ± 19 CPM). An additional 6 transporters were expressed at more than 100 CPM: organic anion-binding protein *Abce1* (153 ± 4 CPM), translation factors *Abcf1* (143 ± 2 CPM), *Abcf2* (152 ± 1 CPM), and *Abcf3* (134 ± 4 CPM), mitochondrial porphyrin transporter *Abcb6* (149 ± 12 CPM), and sterol transporter *Abcg4* (142 ± 6 CPM).

3.1.1.2 | Postnatal Day P8. At P8, 33 transporters were identified; two of these, lipid transporters *Abca4* and *Abca12*, were not present in the adult (<1 CPM), but at P8, these were expressed at 5 ± 0.7 and 1 ± 0.4 CPM, respectively. Two other transporters, which were present in the adult, were not present at P8: multidrug resistance protein *Abcc11* and sterol transporter *Abcg5* (expressed at 2 ± 1 and 3 ± 0.2 CPM, respectively, in P109 animals). Of the highly expressed transporters at P8, innate immune response regulatory gene *Abcf1* (235 ± 13 CPM) was the only one expressed at more than 200 CPM, and 5 others were expressed at >100 CPM (*Abce1*, 144 ± 12 CPM; *Abcf3*, 138 ± 7 CPM; *Abcf2*, 129 ± 9 CPM; multidrug resistance protein *Abcc5*, 121 ± 29 CPM; *Abca2* 102 ± 9 CPM).

Five ABC transporters were more highly expressed in P8 animals than at P109, including lipid transporters *Abca10* (10-fold) and *Abca4* (sevenfold) as well as *Abcc5* (threefold; all p-adj < 0.0001), whereas 19 transporters were significantly lower, including peptide transporter *Abcb9* (11-fold), fatty acid transporter *Abcd2* (ninefold), and *Abca3* (eightfold; all p-adj < 0.0001). The fold change (FC) comparison is summarized in Figure 4 and Table S3.

3.1.1.3 | Postnatal Day P5. In the P5 group, the same 33 transporters were present as in P8 animals, and *Abcf1* remained the highest expressed transcript (232 ± 16 CPM). Three other transcripts had an expression of >100 CPM: *Abce1* (182 ± 10 CPM), *Abcf2* (153 ± 15 CPM), and *Abcf3* (128 ± 5 CPM). *Abcf2* was 1.4-fold lower at P5 compared to P8 animals (p-adj < 0.05).

3.1.1.4 | Postnatal Day P0. At P0, the same 33 transporters were present as in P5 and P8 animals. In addition to *Abcf1*, which was expressed at more than 200 CPM in P5 and P8 animals, another ABC transporter, *Abcf2*, was expressed at 210 ± 49 CPM. Compared to the P5 group, there were three transporters that were significantly higher at P0: *Abcf2*, *Abcc1*, and *Abce1*; however, all changes were relatively small, with none exceeding twofold. Seven ABCs were expressed significantly lower at P0 compared to P5, including sterol transporter *Abcg4* (threefold, p-adj < 0.0001) and lipid transporters *Abca7* (twofold, p-adj < 0.001) and *Abca3* (twofold, p-adj < 0.0001). These comparisons are displayed in Figure 5 and Table S4.

3.1.2 | Inter-Age Comparison

To illustrate any developmental differences in the presence of ABC transporters in the *Monodelphis* brain, datasets from three ages (P0, P8, and P109) were compared. P5 dataset was not included for clarity of the presentation as its transcriptomic profile was very similar to P8 (see above).

Thirty-one of the 35 ABC transporters present in the *Monodelphis* brain were shared among P0, P8, and P109 (Figure 6A). Two transporters, cholesterol transporter *Abcg5* (3 ± 0.2 CPM) and anion transporter *Abcc11* (2 ± 1 CPM), were only found in the P109 group. An additional two transporters were only found in the younger P0 and P8 animals: vitamin A intermediate transporter *Abca4* (5 ± 2 and 5 ± 0.7 CPM, respectively) and lipid transporter *Abca12* (1 ± 0.7 and 1 ± 0.4 CPM, respectively). No transcripts were unique to either P0 or P8 animals.

3.1.3 | Metabolizing Enzymes

Transcripts for a total of 30 metabolizing enzymes were present in the *Monodelphis* brain at P0, P5, P8, and P109. These consisted of 16 cytochrome p450s (CYP), 7 glutathione transferases (GSTs), 3 sulfotransferases (SULT), and 4 uridine 5′-disphosphoglucuronosyltransferases (UGTs). Expression of these enzymes is summarized in Figure 7 and Table S5.

3.1.3.1 | Adult (P109). In P109 brain, there were 22 metabolizing enzymes present. Of these, only *Sult4a1* (597 ± 28 CPM), *Ugt8* (173 ± 26 CPM), and *Gstm3* (164 ± 20 CPM) were expressed at >100 CPM (Figure 7 and Table S5).

3.1.3.2 | Postnatal Day P8. At P8, there were 19 metabolizing enzymes present, with 2 transcripts highly expressed (>100 CPM). These were: *Gstm3* (175 ± 30 CPM), which was also

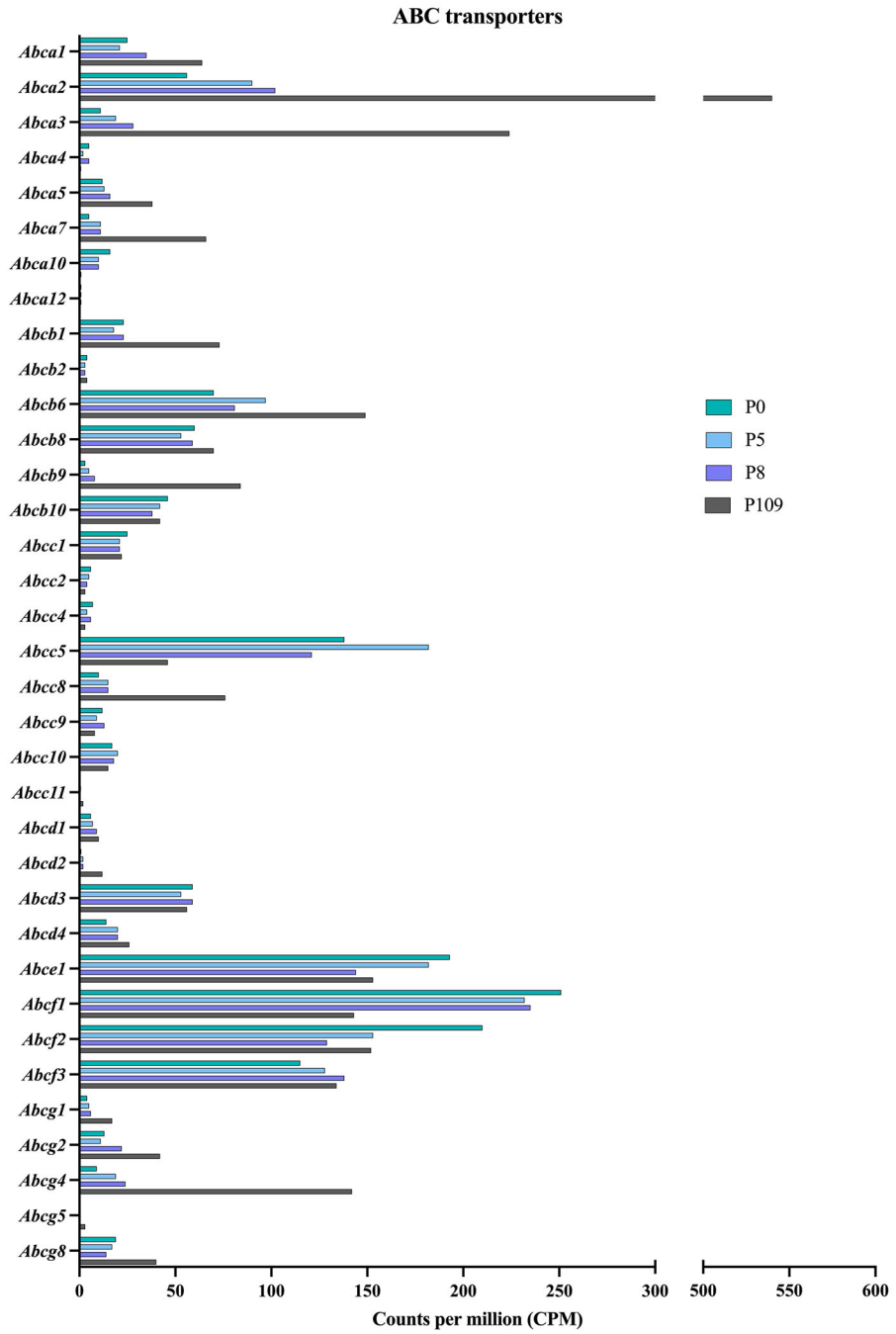

FIGURE 3 | Expression of ABC transporters present in the *Monodelphis* brain at four different ages: P0 (teal), P5 (blue), P8 (purple), and P109 (gray) measured by RNA-sequencing using average normalized counts per million (CPM) from EdgeR analysis. ABC, ATP-binding cassette.

expressed at >100 CPM in P109 animals, and cytochrome p450 oxidoreductase (*Por*; 114 ± 12 CPM). There were 19 enzymes that changed significantly between P8 and P109 (Figure 8 and Table S6). Compared to P109, seven enzymes had significantly higher expression at P8, including *Cyp1b1* (14-fold, p-adj < 0.0001), *Gstcd* (fourfold, p-adj < 0.0001), and UDP-glucose glycoprotein glucosyltransferase 2 (*Uggt2*; fourfold, $p < 0.0001$), whereas 12 transcripts were significantly lower at P8 with large FCs, such as *Ugt8* (350-fold, $p < 0.0001$), *Cyp4f22* (27-fold, p-adj < 0.0001), and *Ugt2a1* (eightfold, $p < 0.05$), as they were not present in P8 animals (<1 CPM).

3.1.3.3 | Postnatal Day P5. Twenty metabolizing enzymes were expressed in P5 brains. Only one transcript was expressed at >100 CPM, *Gstm3* (226 ± 52 CPM), which was also shared with the P8 group. Only *Cyp2s1* expression was significantly different, fivefold (p-adj < 0.05) lower at P5 compared to P8.

3.1.3.4 | Postnatal Day P0. A total of 24 metabolizing enzymes were present in P0 brain, and once again only one, *Gstm3*, was expressed at more than 100 CPM (260 ± 67 CPM). Expression of seven enzymes was significantly changed from P5, with three being significantly lower: *Sult4a1* (threefold,

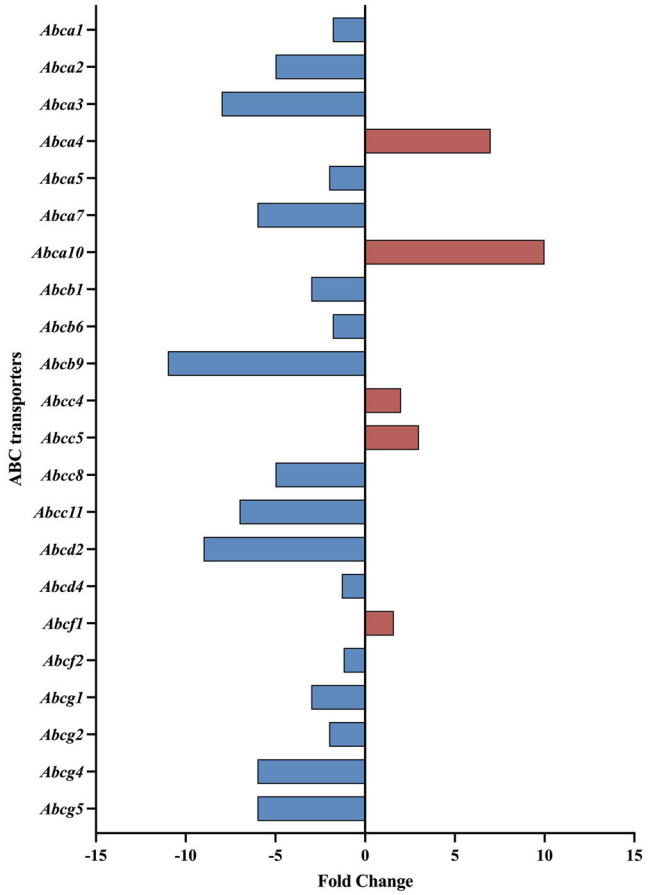

FIGURE 4 | Fold change of ABC transporters in the *Monodelphis* brain at P8 compared to P109. Those that significantly increased (red) or decreased (blue) their expression are displayed. ABC, ATP-binding cassette.

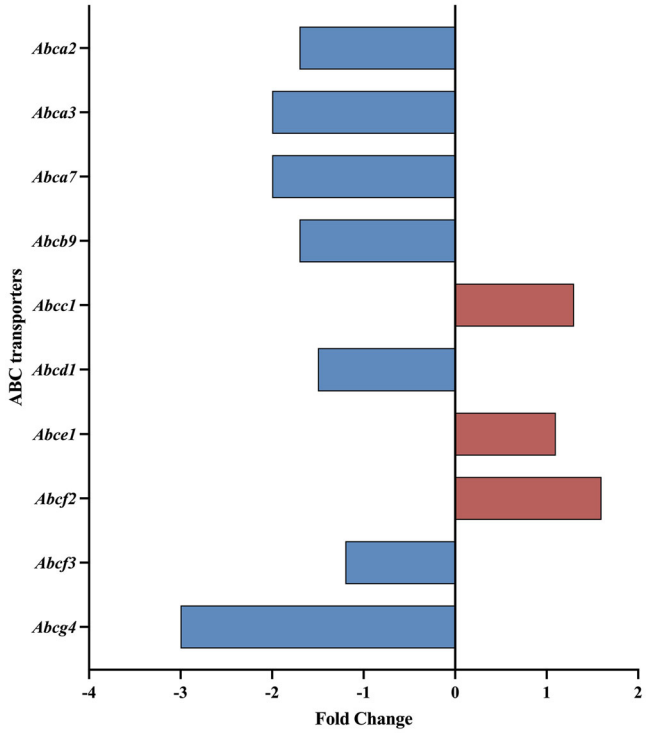

FIGURE 5 | Fold change of ABC transporters in the *Monodelphis* brain at P0 compared to P5. Those that significantly increased (red) or decreased (blue) their expression are displayed. ABC, ATP-binding cassette.

p-adj < 0.0001), *Cyp2d6* (twofold, *p*-adj < 0.01), and *Cyp2u1* (1.5-fold, *p*-adj < 0.05), and four significantly higher: *Mgst1* (twofold, *p*-adj < 0.05), *Cyp2s1* (twofold, *p*-adj < 0.05), *Gstcd* (1.7-fold, *p*-adj < 0.0001), and *Uggt2* (1.5-fold, *p*-adj < 0.0001). Results are displayed in Figure 9 and Table S7.

3.1.3.5 | Inter-Age Comparison. Of the 30 metabolizing enzymes present in the brain, 17 were shared among the three ages (Figure 6B). Four were unique to P0 animals: *Mgst1* (4 ± 2 CPM), *Cyp26c1* (2 ± 2 CPM), *Sult1c3* (2 ± 3 CPM), and *Cyp4v2* (1 ± 0.5 CPM). An additional four transcripts were only found in the P109 group: *Cyp2f1* (2 ± 0.3 CPM), *Ugt2a1* (1 ± 0.6 CPM), *Cyp4f22* (1 ± 0.2 CPM), and *Sult6b1* (1 ± 0.2 CPM). These exclusive genes were all lowly expressed (<5 CPM); no enzyme was found solely in the P8 group. *Ugt8* was only found at P0 and P109 at 1 ± 0.5 and 173 ± 26 CPM, respectively, whereas *Cyp1b1* and *Cyp27c1* were only present at P0 (14 ± 8 and 5 ± 2 CPM, respectively) and P8 (9 ± 6 and 2 ± 0.2 CPM, respectively).

3.1.4 | Solute Carriers

A total of 280 SLCs were present in the *Monodelphis* brain, 26 of which were highly expressed at >200 CPM (displayed in Figure 10 and full list tabulated in Table S8).

3.1.4.1 | Adult (P109). At P109, there were 279 SLCs present. Two SLCs were expressed at more than 1000 CPM: Synaptic vesicle glycoprotein *Sv2a* (*Slc22b1*; 1469 ± 100 CPM) and magnesium transporter *Tusc3* (*Slc58a2*; 1306 ± 80 CPM), and 21 were expressed at over 200 CPM), with three showing expression nearing 1000 CPM: potassium transporter *Slc12a5* (995 ± 50 CPM), gamma-aminobutyric acid:sodium symporter *Slc6a1* (961 ± 50 CPM), and glutamate transporter *Slc1a2* (921 ± 202 CPM). Results are displayed in Figure 10 and tabulated in Table S8.

3.1.4.2 | Postnatal Day P8. In P8 animals, 272 transcripts were present, with 10 expressed at over 200 CPM. These included *Tusc3* (716 ± 90 CPM), ATP:ADP antiporter *Slc25a6* (663 ± 43 CPM), and phosphate transporter *Slc25a3* (549 ± 51 CPM). In addition, a single transcript, nicotinamide adenine dinucleotide (NAD) transporter *Slc25a53*, was expressed at over 1000 CPM (1802 ± 517 CPM). When compared to P109, there were 217 SLCs that changed significantly. Expression of 10 ion transporters, such as *Slc4a5* (129-fold, *p*-adj < 0.0001), *Slc12a1* (97-fold, *p*-adj < 0.0001), and *Slc43a3* (29-fold, *p*-adj < 0.0001), two neurotransmitter transporters: *Sv2c* (18-fold, *p*-adj < 0.0001) and *Slc6a13* (sevenfold, *p*-adj < 0.0001), and an amino acid transporter: *Sfxn2* (threefold, *p*-adj < 0.0001), were among 65 SLCs, which were significantly higher at P8 compared to P109 animals. One hundred and fifty-six transcripts were lower in P8 animals compared to P109 such as glucose:sodium symporter *Slc5a11*, which was 1895-fold lower (*p*-adj < 0.0001), along with 26 ion transporters, including *Slc24a2* (81-fold, *p*-adj < 0.0001), *Slc9c2* (20-fold, *p*-adj < 0.0001), and *Slc9a2* (19-fold, *p*-adj < 0.0001), and 2 amino acid transporters: *Sfxn1* (threefold, *p*-adj < 0.0001)

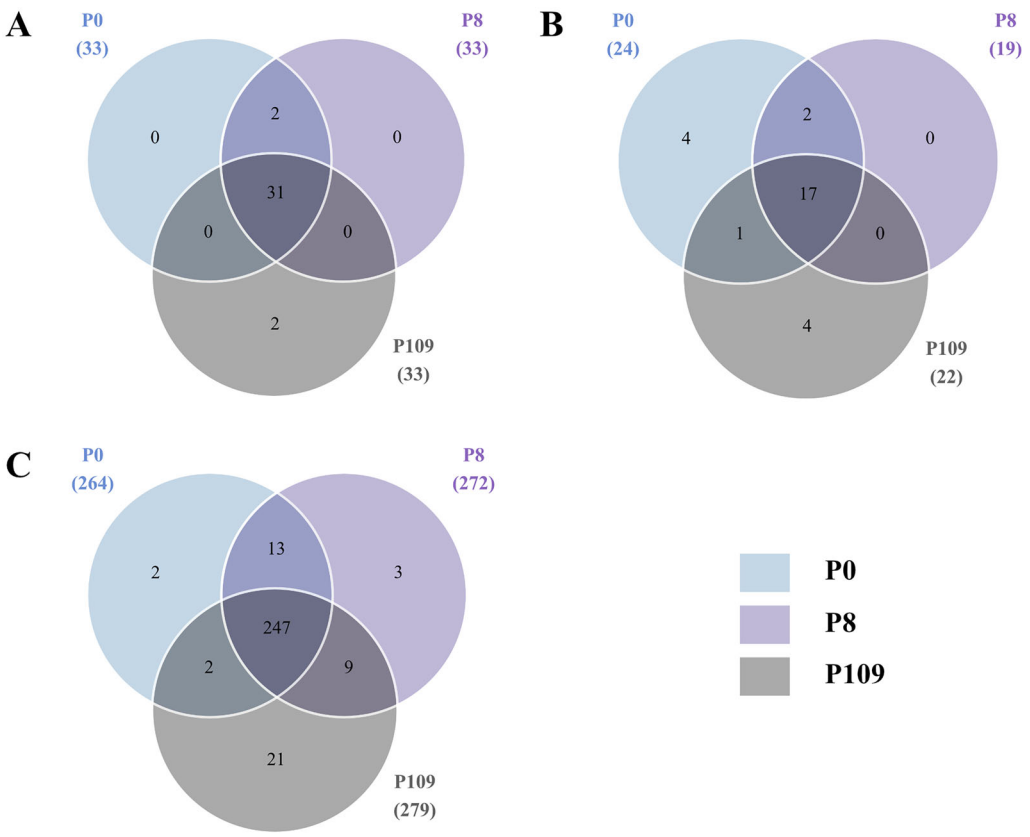

FIGURE 6 | Venn diagram of (A) ABC transporters, (B) metabolizing enzymes, and (C) SLC transporters present in P0 (blue), P8 (purple), and P109 (gray) *Monodelphis* brains identified by RNA-sequencing analysis. Numbers in brackets refer to the total number of individual gene transcripts present in each age group. ABC, ATP-binding cassette; SLC, solute carrier.

and *Sfxn3* (1.4-fold, $p < 0.05$). Four sugar transporters: *Slc35a5* (p-adj < 0.0001), *Slc35a1* (p-adj < 0.01), *Slc35a2* (p-adj < 0.01), and *Slc35a4* (p-adj < 0.05) were also significantly higher in P109 animals compared to P8; however, these changes did not exceed twofold. Significant changes above 10-fold are summarized in Figure 11, and a full list of significant changes is tabulated in Table S9. Functional annotation analysis is displayed in Figure 12.

3.1.4.3 | Postnatal Day P5. At P5, 264 SLCs were present, of which 8 expressed more than 200 CPM, including *Tusc3* (763 ± 65 CPM), *Slc25a3* (559 ± 80 CPM), and *Sv2a* (465 ± 42 CPM). Similar to P8, only *Slc25a53* was expressed at more than 1000 CPM (1157 ± 620 CPM). Compared to the P8 group, there were a total of four transporters that were significantly changed; all were higher at P5. Neurotransmitter transporter, *Slc17a3*, was higher by 14-fold (p-adj < 0.0001), whereas ion transporters, *Slc5a7* and *Slc4a10*, were fourfold and 1.8-fold higher, respectively (both p-adj < 0.05). Sugar transporter, *Slc2a3*, was also 1.7-fold higher (p-adj < 0.05).

3.1.4.4 | Postnatal Day P0. On the day of birth, there were already 264 SLCs present in the neonatal *Monodelphis* brain. Ten of these transporters were expressed at more than 200 CPM, including *Slc25a53* (924 ± 450 CPM), *Slc25a3* (548 ± 91 CPM), and *Tusc3* (502 ± 126 CPM). No transcripts were expressed more than 1000 CPM. A total of 105 SLCs were significantly changed in comparison to the P5 group, with 67 that were significantly lower. Nine of these were ion transporters, including sodium transporters, *Slc13a3* (threefold, p-adj < 0.0001) and *Slc6a15* (1.7-fold), as well as calcium transporters, *Slc24a2* (fourfold, p-adj < 0.01), *Slc24a3* (threefold, p-adj < 0.0001), and *Slc8a2* (twofold, p-adj < 0.0001). Thirty-eight SLCs were significantly higher at P0 compared to P5, including 11 ion transporters, such as sodium *Slco1c1* (10-fold, p-adj < 0.0001), *Slc24a5* (sixfold, p-adj < 0.0001), and *Slc22a3* (fourfold, p-adj < 0.001). Results are summarized in Figure 13 and Table S10 with functional annotation analysis displayed in Figure 14.

3.1.4.5 | Inter-Age Comparison. Altogether, there were 247 SLCs in the brain shared among P0, P8, and P109 animals (Figure 6C). Twenty-one SLCs were only found at P109, including chloride transporter *Slc26a5* (19 ± 2 CPM), *Slc5a11* (19 ± 2 CPM), and dicarboxylate/sulfur oxoanion transporter *Slc25a34* (18 ± 2 CPM), whereas only three transcripts, transmembrane transporter *Slc44a3*, ammonium transporter *Rhcg* (*Slc42a3*), and *Slc5a1*, were unique at P8. In addition, sucrose:proton symporter *Slc45a2* and gamma-aminobutyric acid:sodium symporter *Slc6a12* were only present in the P0 age group. However, these SLCs were all lowly expressed (<3 CPM). There were 13 transcripts that were only shared between the P0 and P8 age groups: sodium:bicarbonate symporter *Slc4a5* (22 ± 24 and 34 ± 19 CPM, respectively), adenine transporter *Slc43a3* (58 ± 26 and 10 ± 2 CPM, respectively), and bile acid:sodium symporter *Slc10a4* (12 ± 4 and 8 ± 2 CPM, respectively), and these were not present at P109 (Figure 6C).

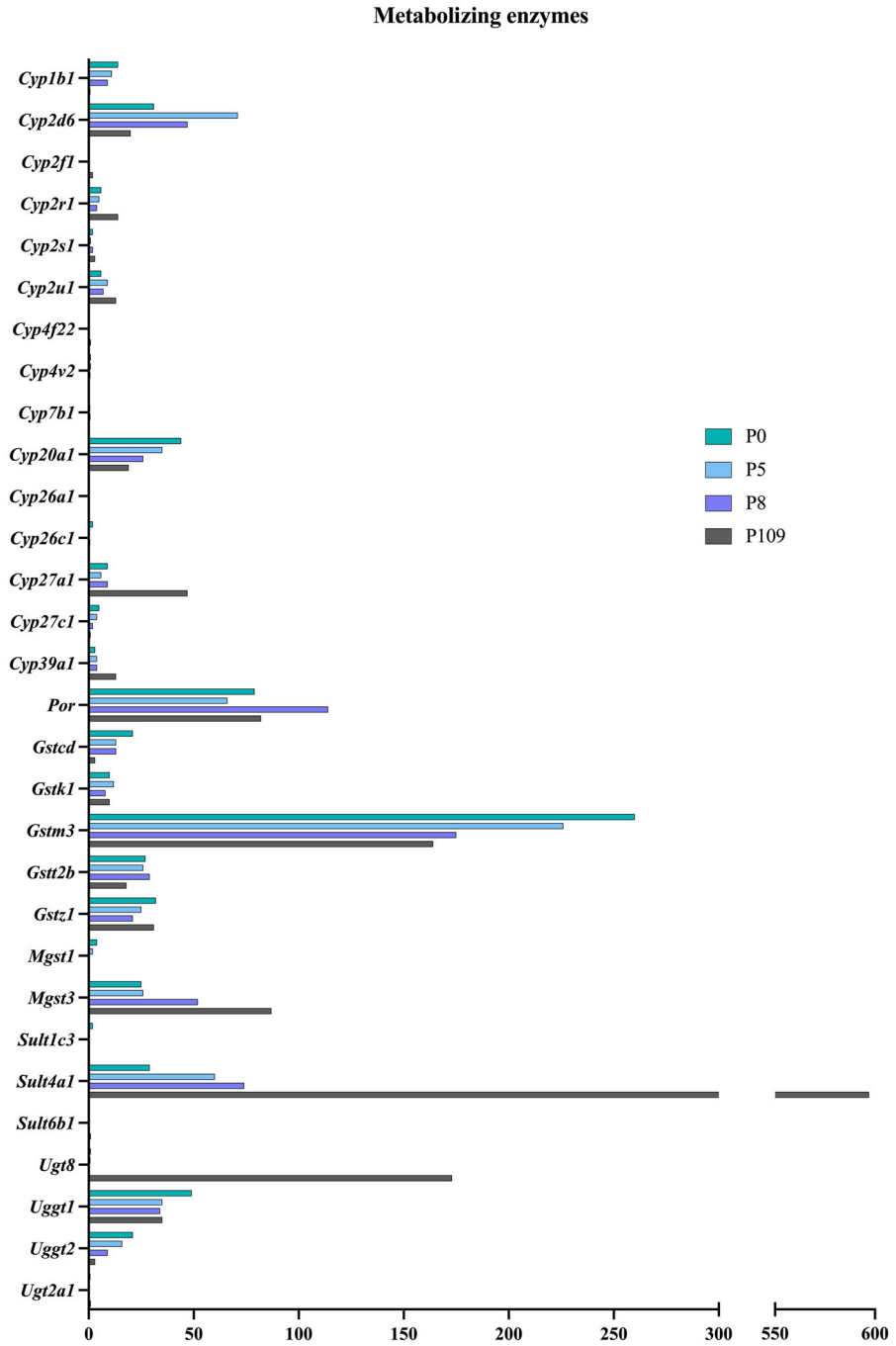

FIGURE 7 | Expression of metabolizing enzymes present in the *Monodelphis* brain at four different ages: P0 (teal), P5 (blue), P8 (purple), and P109 (gray) measured by RNA-sequencing using average normalized counts per million (CPM) from EdgeR analysis.

3.1.5 | Comparison Between *Monodelphis* Newborn Brain and E19 Rat Fetal Brain and Placenta

The hypothesis in the present study was that newborn *Monodelphis* brain may compensate for the lack of placental protection during early brain development by upregulating protective mechanisms from birth, in spite of its extreme immaturity. Therefore, the transcriptomic profile of newborn *Monodelphis* brain in the present study was compared to fetal rat brain and placenta from Koehn et al. (2020) (Figures 15 and 16). A large proportion of ABC and SLC transporters was shared among the three dataset groups (26/43 and 175/358, respectively), whereas the majority of metabolizing enzymes were found in the fetal rat brain and placenta (42/66). In addition, several SLCs and ABC transporters were shared between the E19 rat placenta and P0 *Monodelphis* brain, and 8 out of the 14 identified transcripts were also found in the adult rat brain (Koehn et al. 2021). These transporters, *Slc2a3*, *Slc2a12*, *Slc16a3*, *Slc5a5*, *Slc37a2*, *Slc25a35*, *Slc16a4*, and *Slc22a3*, are involved in the transport of a variety of molecules, including sugars, monocarboxylic acids, and drugs.

Overall, although there were some transcripts that were only found in the *Monodelphis*, a greater overall number of transcripts were identified in the rat compared to the *Monodelphis* in every

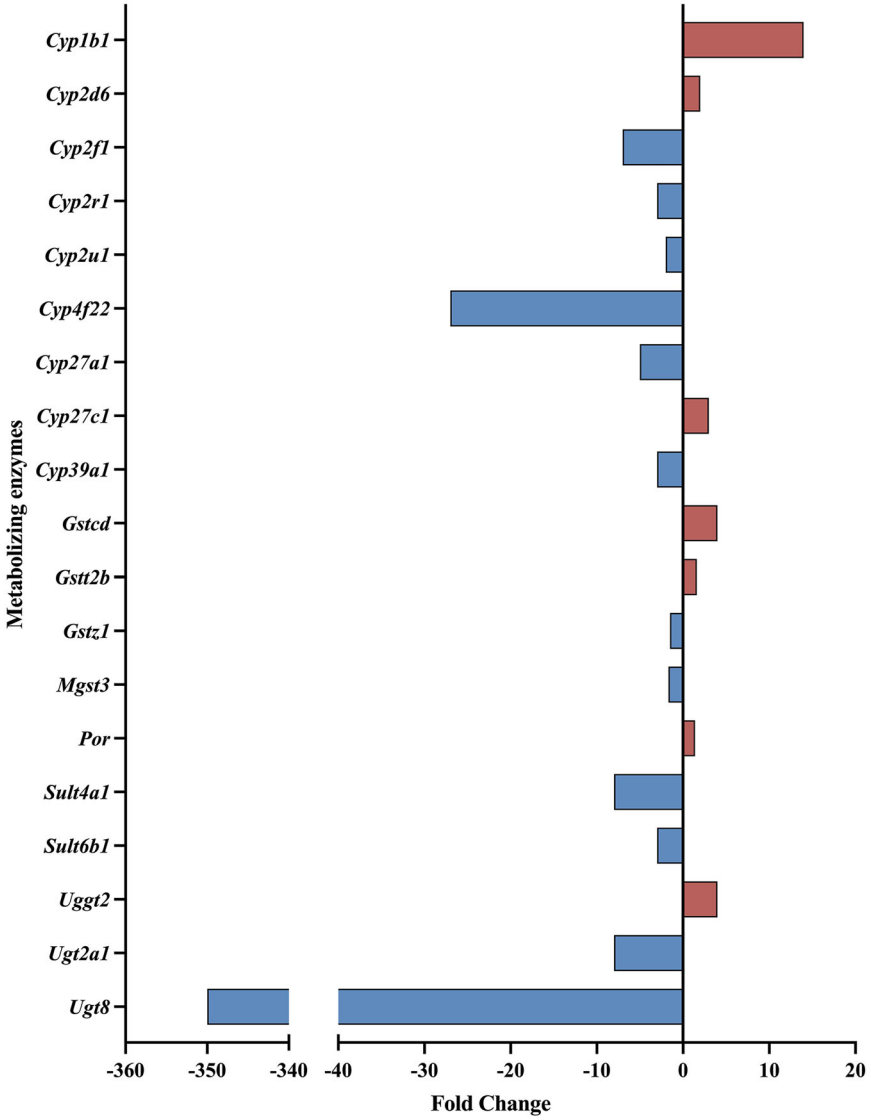

FIGURE 8 | Fold change of metabolizing enzymes in the *Monodelphis* brain at P8 compared to P109. Those that significantly increased (red) or decreased (blue) their expression are displayed.

category investigated (Table S1). Among the ABC transporters, 49 were found in the rat, compared to 41 in the *Monodelphis*. For metabolizing enzymes, 139 were detected in the rat dataset and 44 in the *Monodelphis* dataset, whereas 430 SLCs were found in the rat and 362 were found in the *Monodelphis*. This may well be the outcome of *Monodelphis* genome being less well annotated than that of the rat (see Section 4). Figure 16 displays the number of transcripts that were present (>1 CPM) in each category.

3.2 | Entry of Paracetamol Into the Developing Brain and CSF

To test the overall functionality of the transporters in the developing *Monodelphis* brain, the entry of paracetamol from the circulation into the brain and CSF was investigated at five developmental ages: P5, P8, P28, P62, and P110/113 (combined as P110).

Paracetamol transfer into the cortex and CSF was the highest in the youngest brain tested (P5) and dropped from 75% ± 3% (brain) to 62% ± 2% (CSF) at P5 to around 50% in both compartments at P8 ($p < 0.01$ and $p > 0.05$, respectively). From then on, it remained at the level of around 40%–50% until P110. There was no difference between paracetamol entry into the brain and the CSF at any age ($p > 0.05$). Results are listed in Table 2 and shown in Figure 17A,B, with statistical significance displayed. Data show that *Monodelphis* brain barriers, even at this very early stage of development, were already able to restrict (less than 100%) the entry of paracetamol from circulation into the brain and CSF (see Section 4).

3.2.1 | Interspecies Comparison: Rat and *Monodelphis*

Drug entry into the brain and CSF in *Monodelphis* can be compared with the eutherian rat using previous published data (Koehn et al. 2019), although it is difficult to accurately match stages of brain developments across species (see above and Saunders et al. 1989). In both species, the transfer of paracetamol into the brain and CSF was higher in the younger animals and

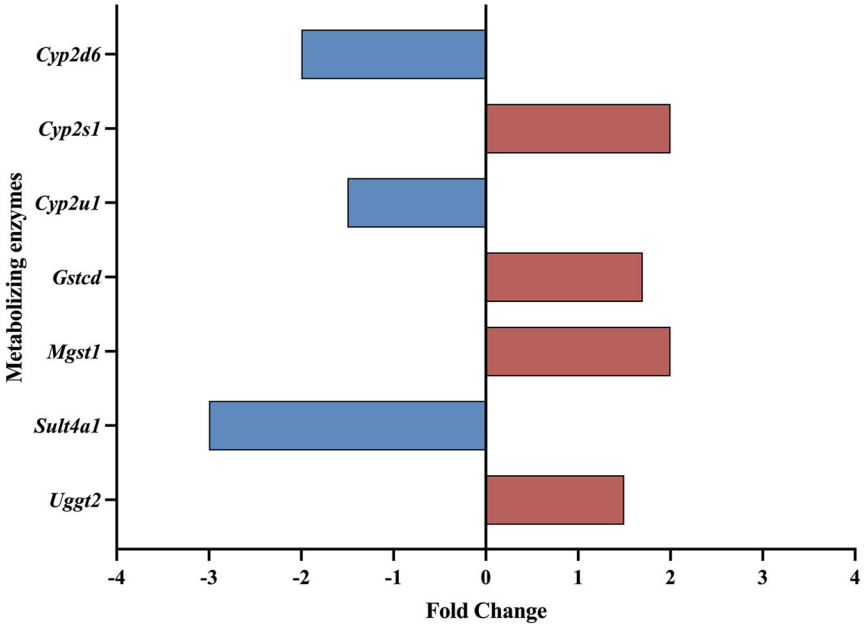

FIGURE 9 | Fold change of metabolizing enzymes in the *Monodelphis* brain at P0 compared to P5. Those that significantly increased (red) or decreased (blue) their expression are displayed.

TABLE 2 | Cortex/plasma and cerebrospinal fluid (CSF)/plasma concentration ratios (%) and number of animals used at five ages: P5, P8, P28, P62, and P110 following a single intraperitoneal (*i.p.*) injection of 15 mg/kg paracetamol along with its radiolabelled tracer [^{3}H]-paracetamol.

Ages	*n*	μCi	Cortex/Plasma	CSF/Plasma
P5	3	0.33	75 ± 3	62 ± 2
P8	5	0.33	46 ± 16**	49 ± 10
P28	4	0.5	57 ± 5	55 ± 2
P62	4	0.5	37 ± 8**	44 ± 5**
P110	3	2.5	44 ± 5*	45 ± 3*

Note: The number of animals used at P5 refers to the number of pooled samples; each pool contained samples from two to three animals. The amount (μCi) of [^{3}H]-paracetamol included in each injectate at each age is also depicted; note that the concentration of paracetamol in the radiolabel is present in trace amounts only; *$p < 0.05$, **$p < 0.001$.

decreased with age (Figure 17A,B). However, entry into the brain was higher in the newborn P5 *Monodelphis* (75% ± 3%) than in E19 rat (46% ± 5%, $p < 0.001$), as shown in Figure 17A. A similar trend was observed in the CSF, with 62% ± 2% of paracetamol transferring into P5 *Monodelphis* CSF compared to 40% ± 7% in the E19 rat ($p < 0.001$, Figure 17B).

3.3 | Distribution of Paracetamol in the *Monodelphis* Brain

Autoradiography was used to visualize the distribution of paracetamol in the *Monodelphis* brain in P8 and P100 animals, which were exposed to a single *i.p.* injection of [^{3}H]-paracetamol (Figure 17C–H). Brain sections from untreated control P8 and P100 animals with no injected radioactivity (Figure 17C,D) were developed alongside the treated brains (Figure 17E,F) to display the background level of radioactivity. In all cases, the radioactivity in these control brains was below the level of quantification (^{3}H standards, Figure 17G,H). In the brains of animals exposed to [^{3}H]-paracetamol, radioactivity was relatively uniformly distributed throughout the brain at both ages; however, the intensity of radioactivity in P8 *Monodelphis* brain was much higher than that in P100 brain (Figure 17E,F). Some possible reasons for this difference are considered in Section 4.

4 | Discussion

In the present study, *M. domestica* was chosen due to its very early developmental stage at birth, allowing for investigations of an animal that develops almost entirely ex utero without the extra protection of the placenta. *Monodelphis* are born at an embryonic stage of brain development compared to eutherian mammals. The gestational period lasts only 14 days, with a transient placenta present for only the few final days before birth (Saunders et al. 1989). However, many developmental features are comparable between marsupials and eutherians. In both *Monodelphis* and rat, studies investigating the integrity of blood–brain barriers have found that tight junctions are already present and functional early in development (Habgood et al. 1993; Ek et al. 2003, 2006). The total protein concentration in plasma increases with age until adulthood, whereas concentration in the CSF peaks at around P8–P10 in the *Monodelphis* and just before birth in the rat (Dziegielewska et al. 1981, 1989).

We used *Monodelphis* to investigate the transcriptomic profiles of ABC transporters, metabolizing enzymes, and SLCs in the brain at four ages: P0, P5, P8, and juvenile (P109) using RNA-Seq. In addition, the levels of brain and CSF entry of paracetamol during development were estimated using liquid scintillation counting, and distribution was determined using autoradiography. Results

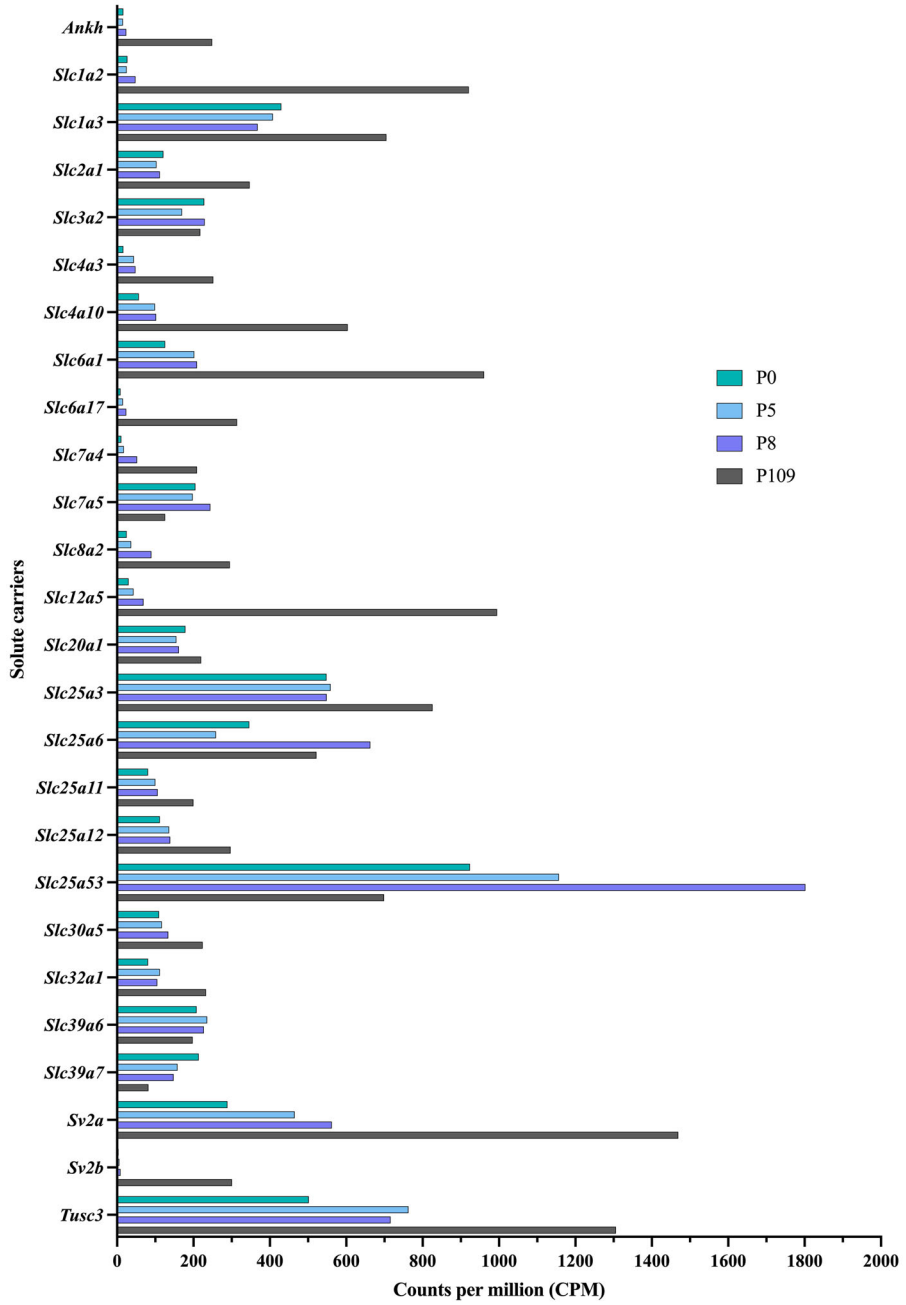

FIGURE 10 | Expression of solute carriers (SLCs) present in the *Monodelphis* brain at four different ages: P0 (teal), P5 (blue), P8 (purple), and P109 (gray) measured by RNA-sequencing using average normalized counts per million (CPM) from EdgeR analysis. Note that only SLCs present at >200 CPM at any developmental age are included in this figure. The full list is displayed in Table S8.

were then compared with previous data obtained from the rat (Koehn et al. 2019, 2021; Huang et al. 2023) in order to shed light on the differences between mechanisms protecting the brain when it develops with or without placental protection.

4.1 | Transcriptomic Changes During Brain Development

Overall, the transcriptomic profiles of P0, P5, and P8 brains were more similar to each other than the P109 brain profiles. The number of significant changes between the age groups was consistently higher in the P8 versus P109 age group compared to P0 versus P5 in the transcripts investigated. Furthermore, the magnitude of the FC did not surpass 10-FC between P0 and P5 animals, whereas between P8 and P109, 30 transcripts exceeded this threshold, with several reaching over 50-FC (e.g., Figure 13 compared to Figure 11). There were also a few significant differences, some of which were intensified in P109 animals. An example is lipid transporter *Abca2*, which increased from 56 ± 4 CPM at P0 to 102 ± 9 CPM at P8 to become the highest expressed ABC transporter in P109s at 540 ± 22 CPM in *Monodelphis* (Figure 3). The same trend was observed in the rat, where *Abca2* transcript numbers showed a stepwise increase from E19 fetuses (119 ± 8 CPM) to adults (409 ± 126 CPM; Huang et al. 2023).

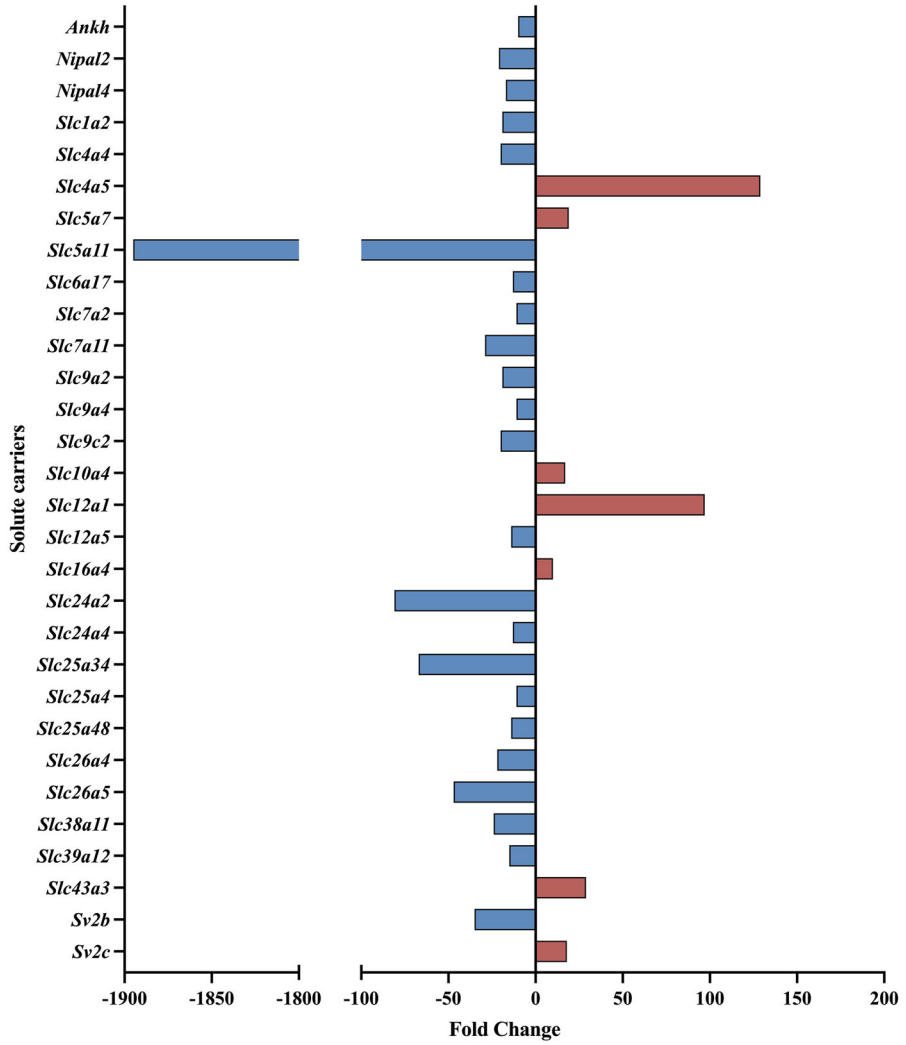

FIGURE 11 | Fold change of solute carriers (SLCs) in the *Monodelphis* brain at P8 compared to P109. Those that significantly increased (red) or decreased (blue) their expression are displayed. Note that only comparisons of transporters with more than 10-fold change are included. The full list is available in Table S9.

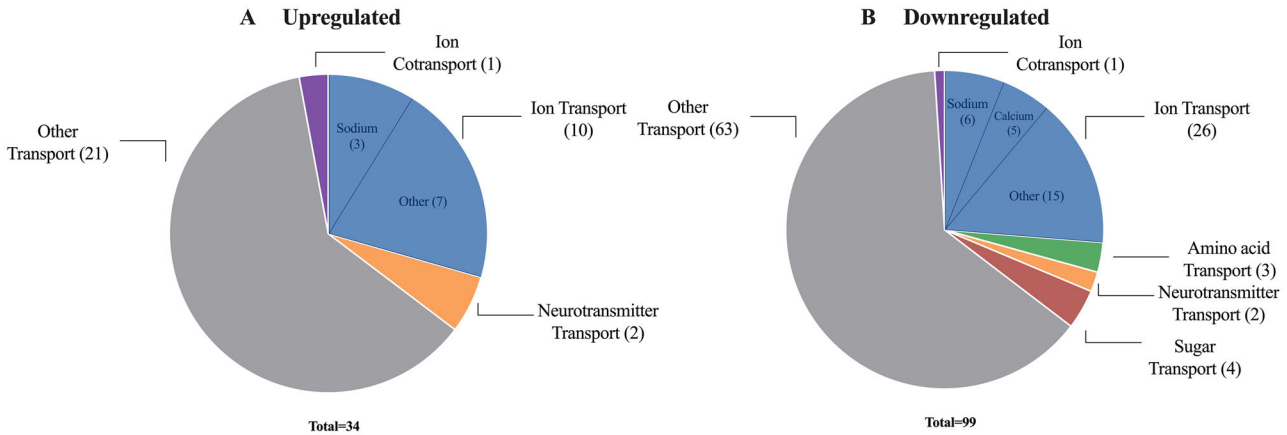

FIGURE 12 | Chart of (A) upregulated and (B) downregulated solute carriers (SLCs) with transporter function in the *Monodelphis* brain at P8 compared to P109. Functional annotation of biological processes conducted using DAVID (UniProtKW). Numbers in brackets refer to the number of individual gene transcripts present in each category. Total, number of individual gene transcripts included in each analysis.

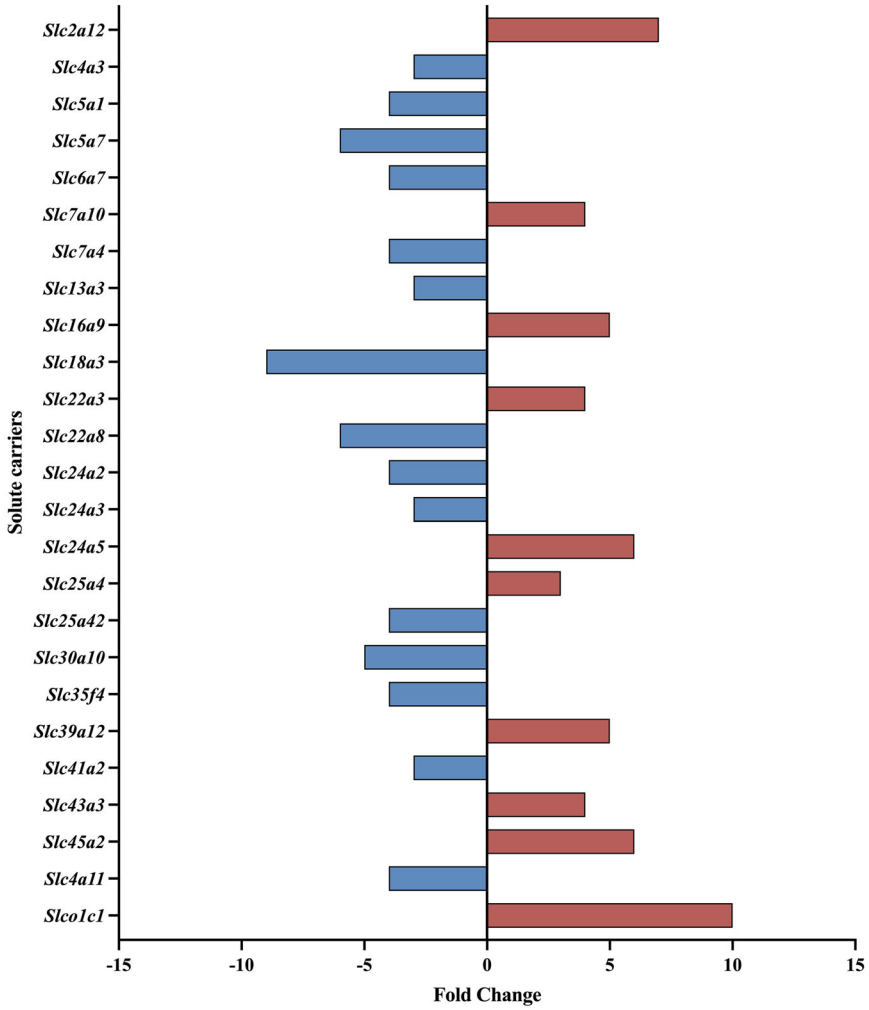

FIGURE 13 | Fold change of solute carriers (SLCs) in the *Monodelphis* brain at P0 compared to P5. Those that significantly increased (red) or decreased (blue) their expression are displayed. Note that only comparisons of transporters with more than a 3-fold change are included. The full list is available in Table S10.

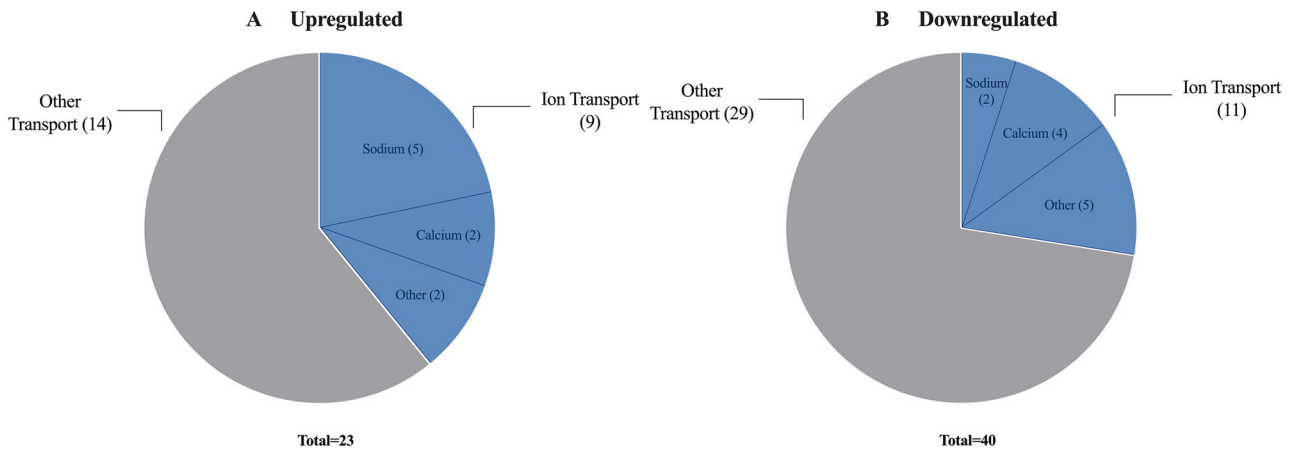

FIGURE 14 | Chart of (A) upregulated and (B) downregulated solute carriers (SLCs) with transporter function in the *Monodelphis* brain at P0 compared to P5. Functional annotation of biological processes conducted using DAVID (UniProtKW). Numbers in brackets refer to the number of individual gene transcripts present in each category. Total, number of individual gene transcripts included in each analysis.

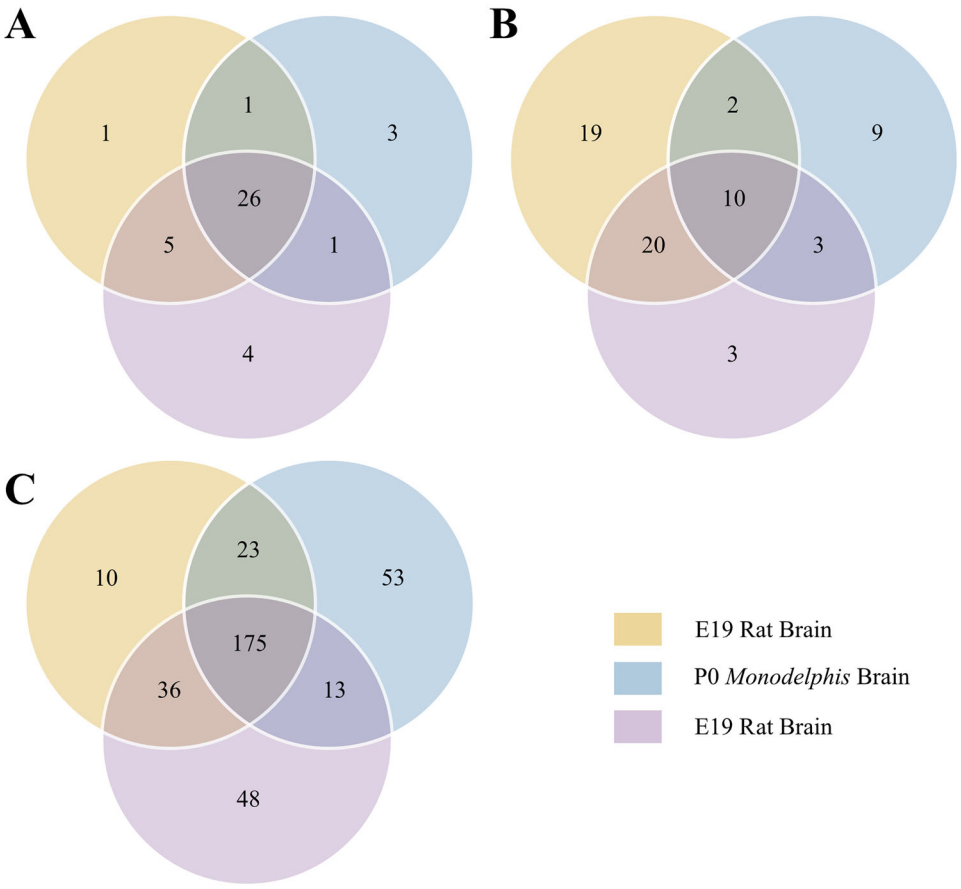

FIGURE 15 | Venn diagram of (A) ABC transporters, (B) metabolizing enzymes, and (C) solute carriers (SLCs) present in the E19 rat brain (yellow), P0 *Monodelphis* brain (blue), and E19 rat placenta (purple) identified by RNA-sequencing analysis. Numbers in brackets refer to the total number of individual gene transcripts present in each age group. ABC, ATP-binding cassette.

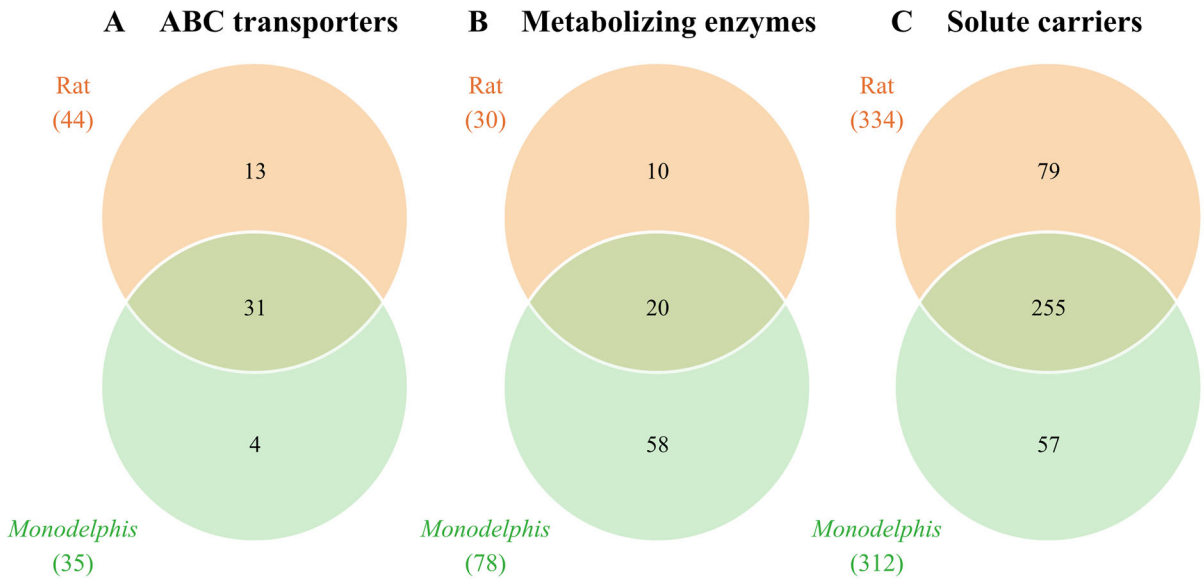

FIGURE 16 | Number of (A) ABC transporters, (B) metabolizing enzymes, and (C) solute carriers (SLCs) present in the rat (orange) or *Monodelphis* brain (green; combined ages). Number in brackets refers to the total number of individual gene transcripts present in each species. ABC, ATP-binding cassette.

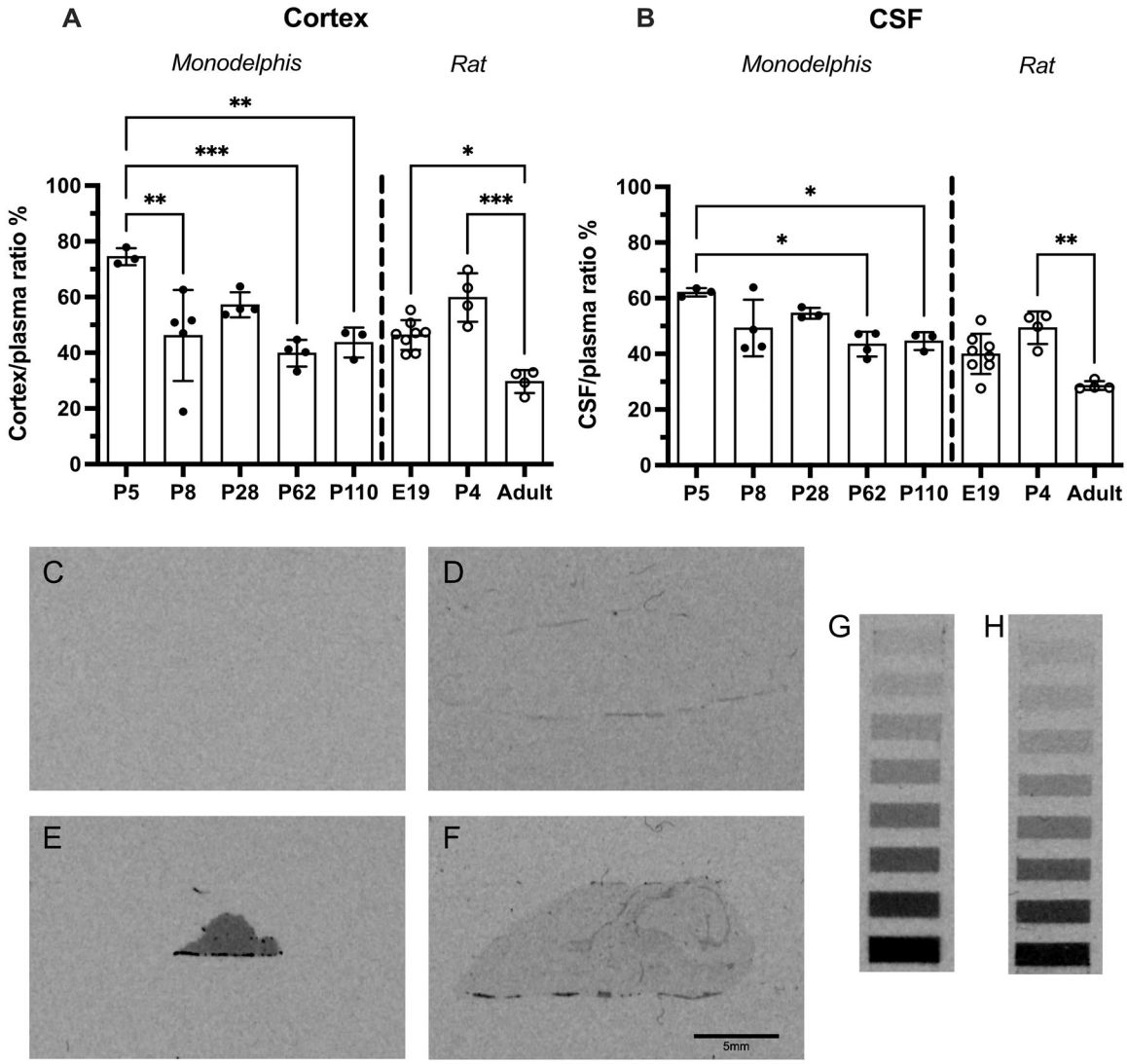

FIGURE 17 | Entry of [^{3}H]-paracetamol in the *Monodelphis* and rat into the (A) brain cortex and (B) CSF 30 min after a single intraperitoneal (*i.p.*) injection of 15 mg/kg paracetamol. *Monodelphis* at five ages: P5, P8, P28, P62, and P110, and rat at three ages: E19, P4, and adult (7- to 8-week-olds) were used. Means ± SD. Each point represents an individual animal, except in P5 *Monodelphis*, where each point is a pooled sample from two to three animals. *$p > 0.05$, **$p < 0.01$, ***$p < 0.001$. Autoradiographic images of sagittal sections of *Monodelphis domestica* brains in (C) untreated control P8, (D) untreated control P100, (E) P8 treated with a single dose of paracetamol (15 mg/kg) along with 0.33 μCi [^{3}H]-paracetamol, (F) P100 treated with a single dose of paracetamol (15 mg/kg) along with 5 μCi [^{3}H]-paracetamol. (G and H) Radioactive ^{3}H standards (Amersham, 3.1–35 ng/mg): (G) P8 and (H) P100; these standards were exposed on the same films as their respective brain sections. Brains in (C) and (D) were not exposed to radioactivity and only show background levels of radioactivity. Scale bar in the bottom right of (D) is 5 mm and applies to all images. Note the difference in intensity of radioactivity between the two ages, neither having specific regional accumulation. Two films were used to create these autoradiograms: (C), (E), and (G) were developed on one film, and (C), (F), and (H) were developed on the second film. Note that the background density in (C) (P8 control) is below the lowest standard in (G). CSF, cerebrospinal fluid. *Source*: (A and B) Rat values are from Koehn et al. (2019).

This increase in the transcripts in the mature brain compared to early developing brain probably reflects the extreme immaturity of *Monodelphis* at the time of birth (Saunders et al. 1989; Workman et al. 2013).

4.1.1 | Interspecies Comparison

Interspecies comparisons are generally difficult without specifying which organ or its part is being compared. For example, *Monodelphis* pups are born at an embryonic stage of cortex development (Saunders et al. 1989; Cardoso-Moreira et al. 2019), whereas their brainstem is much more advanced, which allows breathing and suckling that are essential for survival at birth (Saunders et al. 1989). Cortex of a newborn *Monodelphis* is more like E12–13 rat than E19 rat (Saunders et al. 1989; Cardoso-Moreira et al. 2019). P8 *Monodelphis* cortex corresponds to about E15–16 rat, whereas the 7-week-old rat (adult) and P110 *Monodelphis* are at similar stage of development (Saunders et al. 1989). This highlights the usefulness of marsupials for studies of early stages of brain development. Nevertheless, brains from both species at around the time of birth are here discussed for a comparative

purpose using rat data from Koehn et al. (2020, 2021) and Huang et al. (2023).

Overall, there were more ABC transporter transcripts found in the rat brain (Figure 16). However, it is unclear whether this is a true representation of the number of transcripts present in *Monodelphis* due to the much more limited annotation of the genome of this species; these values also include all transcripts detected, not just those reaching >1 CPM. Therefore, only a comparison of overall developmental trends between rat and *Monodelphis* is discussed here. Some studies have explored true cross-species analysis of RNA-Seq data (e.g., LoVerso and Cui 2015) using a combined genome annotation, but this analysis is beyond the scope of the present study.

In the *Monodelphis*, most ABC transporters were equally or more highly expressed at P109 compared to the younger ages, with only a handful of exceptions, including *Abcc5* and *Abcf1*. *Abcc5* is a ubiquitous efflux transporter involved in exporting cyclic nucleotides (Dazert et al. 2003; Meyer zu Schwabedissen et al. 2005), and *Abcf1* takes part in regulating the innate immune response, both contributing to drug efflux (Wilcox et al. 2017). This was not seen in the rat datasets, as expression of *Abcc5* was similar between fetal and adult brains, whereas *Abcf1* was more highly expressed in the younger animals. However, in the E19 rat placenta, *Abcf1* expression was the highest compared to rat brain or choroid plexus at any age. This reinforces the proposition that it could be the level of expression (or functionality) of individual transporters that may protect *Monodelphis* brain during its development ex utero from a much more immature stage than in any eutherian animal. SLCs in *Monodelphis* were highly expressed, with 10 transcripts exceeding 500 CPM, whereas only 2 ABC transporters or their metabolizing enzymes (*Abca2* and *Sult4a1*) reached this level of expression. A similar pattern was observed in the rat, with the expression of SLCs generally higher than both ABC transporters and metabolizing enzymes (Huang et al. 2023). Additionally, the neonatal (P5) *Monodelphis* brain was also compared to the fetal (E19) rat brain (Figure 15) to determine if the newborn *Monodelphis* may be able to compensate for the lack of placental protection during brain development. Several transporters, which were found in the E19 rat placenta and P0 *Monodelphis* brain but not in the E19 rat brain, were also found in the adult rat brain. This implies that they play a role in the brain, but during development in eutherians, they are present in the placenta instead of fetal brain.

4.1.2 | Entry and Distribution of Paracetamol Into the Developing *Monodelphis* Brain

The entry of paracetamol in *Monodelphis* was measured at five developmental ages following a single-drug dose. Paracetamol entry into both the brain and CSF was highest in the youngest (P5) experimental animals (75% ± 3% and 62% ± 2%, respectively) before dropping to around 50% and remaining relatively stable from P8 through to P110 (Figure 17A,B). Autoradiograms of P8 and P100 brains (Figure 17E,F) showed a higher intensity of radioactivity in the newborn brain. This was likely due to a combination of higher [^{3}H]-paracetamol entry into the brain (Figure 17A,B) as well as a higher amount of injected radioactivity per body weight (approximately 50 times, see Section 2), mostly due to the difficulty of injecting very small volumes into such small animals. The previously described distribution of paracetamol in the early postnatal (P4) rat brain (Koehn et al. 2021) appears to be equally dispersed to that observed in P8 *Monodelphis* (Figure 17E); however, distribution in the adult rat brain appears to be different to the one observed in *Monodelphis*. In the rat, a very clear distribution of paracetamol was visible confined to white matter tracts (Koehn et al. 2021), whereas in *Monodelphis*, such accumulation was not observed (Figure 17E,F). This difference could be due to species differences in myelination tracts between mammalian and marsupial brains, as has been described previously (Saunders et al. 1989).

Compared to the rat, entry of paracetamol was higher in *Monodelphis* in general (Figure 17A,B) but showed some restriction (less than 100% brain/plasma ratio), potentially due to drug efflux, even in the newborn. Higher brain entry in *Monodelphis* compared to the rat could be explained by paracetamol being a weaker substrate for any of the transporters in *Monodelphis*. Another possible explanation might be the distinct lack of metabolizing enzymes found in the early *Monodelphis* brain (Figure 16). For example, in the case of paracetamol, of the metabolizing enzymes known to be involved in transport by ABC efflux transporters (Mazaleuskaya et al. 2015), only *Sult1a1* was present at any age investigated in *Monodelphis*. In addition, in the minor metabolic pathway leading to excretion via urine, only *Cyp2d6* and *Gstm1* were present, which facilitate the formation of *N*-acetyl-*p*-benzoquinone-imine (NAPQI) and paracetamol-glutathione, respectively (Mazaleuskaya et al. 2015). Therefore, it is possible that paracetamol and its metabolites are kept within the brain tissue for longer in *Monodelphis* than in the rat. Nevertheless, the lower entry of paracetamol into fetal rat brain compared to early *Monodelphis* neonate brain reinforces the importance of the placental protection in limiting the exposure of the developing CNS to potentially harmful substances.

4.1.3 | Effects of the Placenta on Drug Entry

In the present study, paracetamol was always injected *i.p.* directly to the pups, whereas in previous rat studies, the drug was administered either to the rat dam (intravenous [*i.v.*]) with the fetuses only exposed to the drug via maternal circulation or directly (*i.p.*) to the rat fetus, therefore bypassing the placental interface (Figure 18). Therefore, for comparative purposes, Figure 18 includes brain entry of paracetamol in the neonatal *Monodelphis* (P5) after *i.p.* injection and rat brain entry at E19 after either *i.p.* injection or *i.v.* injection to the dam. Entry of paracetamol in both the brain cortex and CSF was highest in P5 *Monodelphis* (75% ± 3% and 62% ± 2%, respectively) and lowest in rats that were exposed through the dam (28% ± 9% and 25% ± 8%, respectively). This difference most likely reflects the limiting effect of the placenta on the drug transfer into the developing brain of a eutherian mammal.

4.1.4 | Conclusions

The hypothesis in the present study was that newborn *Monodelphis* brain may compensate for the lack of placental protection during early brain development by upregulating the expression

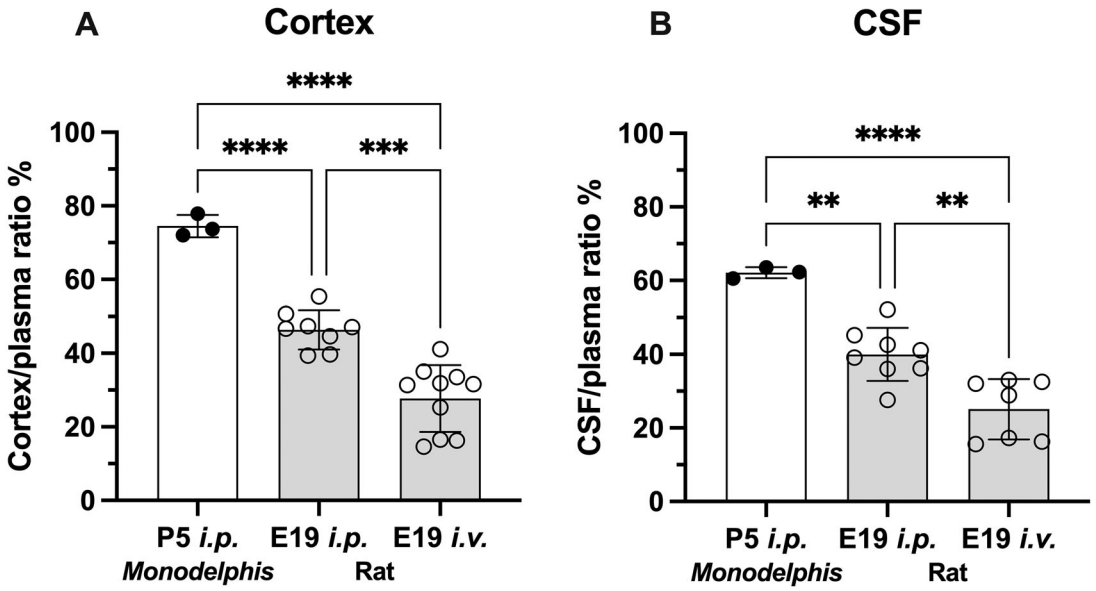

FIGURE 18 | Entry of [^{3}H]-paracetamol in P5 *Monodelphis* and E19 rat into the (A) brain cortex and (B) CSF 30 min after a single intraperitoneal (*i.p.*) or intravenous (*i.v.*) injection of 15 mg/kg paracetamol. Paracetamol entry into the brain and CSF for both *i.v.* and *i.p.* administration was calculated in comparison to fetal plasma. Means ± SD. Note that each point is an individual animal. $^{**}p < 0.01$, $^{***}p < 0.001$, $^{****}p < 0.0001$. *i.p.* rat values, unpublished study. CSF, cerebrospinal fluid. *Source: i.v.* rat values obtained from Koehn et al. (2019).

of protective mechanisms from birth, despite its extreme immaturity. Indeed, there were several ABC transporters, metabolizing enzymes, and SLCs that were shared between the E19 rat placenta (but not its brain) and P0 *Monodelphis* brain (Figure 15), and 8/14 transcripts identified in E19 rat placenta and P0 *Monodelphis* brain were also found in the adult rat brain (Koehn et al. 2021). This finding indicates that these transporters do play a role in the brain, but in eutherians, during early stages of development, they are present in the placenta instead of fetal brain.

Physicians are hesitant to prescribe drugs to pregnant women, but some medications cannot be stopped during pregnancy, including those that treat serious conditions such as epilepsy or neuropsychological conditions. In the case of paracetamol, its transient use may be essential to modify the deleterious effects of fever on the developing fetus (Dreier, Andersen, and Berg-Beckhoff 2014). In our previous studies, the rat was used as a eutherian animal model to investigate the entry of analgesic/antipyretic drug, paracetamol, into the developing brain and CSF, including during pregnancy (Koehn et al. 2019). Possible cellular mechanisms involved in drug entry across brain and placental barriers were also investigated using a transcriptomic analysis of ABC and SLC transporters (Koehn et al. 2021; Huang et al. 2023). Results obtained highlighted the contribution of the placenta in controlling drug entry into the fetal brain. In the present study, a marsupial, the gray short-tailed opossum, *M. domestica*, was used as an example of an animal that develops almost entirely ex utero. The experiments described here showed that the entry of paracetamol was higher in *Monodelphis* than in the rat at all ages. Entry of the drug into the brain and CSF at P5 *Monodelphis* was significantly higher than in the E19 fetal rats, especially when the drug was administered via the dam (Figure 17A,B), indicating the importance of the placenta in reducing the drug entry from maternal circulation into the eutherian developing brain.

There is an interesting evolutionary aspect to the identification of efflux mechanisms in rat and *Monodelphis*. These species will not have been exposed to paracetamol or other drugs in their early evolution. The presence of effective drug efflux mechanisms presumably reflects early exposure to environmental toxins that share some commonality with drugs. Further consideration of this is outside the scope of this article.

4.1.5 | Limitations of the Study

1. Identity of efflux and influx transporters in the present study was established using transcriptomic analysis. Although quite comprehensive, the annotation of *Monodelphis* genome is less complete than that of the rat or human; therefore, it is possible that identification of some transcripts was missed.
2. As discussed previously (Koehn et al. 2021; Huang et al. 2023), the correlation between gene expression and their gene–protein product distribution is not well understood as upregulated/downregulated genes are not always reflected in an increase/decrease in the corresponding protein activity (Greenbaum et al. 2003; Liu, Beyer, and Aebersold 2016). To test the functionality of these transporters, the brain entry of paracetamol was investigated across development by establishing the baseline level of its entry. However, as it was not possible to make a correlation between drug brain entry data and the expression of various transporters directly, therefore, further investigations in measuring protein levels of these transporters and enzymes may be necessary to fully elucidate the specific mechanisms determining the entry of each drug across various cellular barriers.
3. Several transporters are known to have more than one molecular form, depending on the animal species. For example, Pgp has two forms in the rat: *Abcb1a* and *Abcb1b*, whereas in the

human and *Monodelphis*, a single *Abcb1* gene is present (Safran et al. 2021). Many transporters, including ABC transporters, are, however, well conserved across mammalian species, for example, Abcc1 has 85% similarity between the rat and *Monodelphis* in amino acid sequence (Safran et al. 2021). Nevertheless, care should be taken when translating results across species; further studies investigating the correlation between species would be beneficial.

4. Only a single drug was tested for its brain entry. For a more comprehensive comparison with eutherian species, such functional studies ought to be extended to more test substances. In addition, the present experiments were all acute; therefore, it is not possible to answer the question if transporters' expression in *Monodelphis* can be modified when exposed to the drug over a prolonged period, as has been shown for the rat (Koehn et al. 2021; Huang et al. 2023) and is well known in some cases of cancer treatment regimes in human (e.g., Eckford and Sharom 2006; Sedláková et al. 2015).

Author Contributions

Y.H., N.R.S., and J.L.V. are responsible for the initiation of the study. Most of the experimental work was done by Y.H., A.C.C.L. was involved in RNA-sequencing. All authors contributed to writing the manuscript. P.D.C. was responsible for autoradiography development. Y.H. travel to Texas was supported by Monash Study Away.

Ethics Statement

All experimental work was approved by local Animal Ethics Committees: University of Melbourne Ethics Committee (Ethics Approval AEC: 10270) and The University of Texas Rio Grande Valley IACUC (Protocol AUP-22-07).

Conflicts of Interest

The authors declare no conflicts of interest.

Data Availability Statement

The data that support the findings of this study are openly available in NCBI at https://www.ncbi.nlm.nih.gov/bioproject/PRJNA1052735, reference number PRJNA1052735.

Peer Review

The peer review history for this article is available at https://publons.com/publon/10.1002/cne.25655.

References

Australian Medicines Handbook. 2022. *Australian Medicines Handbook 2022*. Adelaide: Australian Medicines Handbook Pty. Limited.

Blazquez, A. G., O. Briz, E. Gonzalez-Sanchez, M. J. Perez, C. I. Ghanem, and J. J. G. Marin. 2014. "The Effect of Acetaminophen on the Expression of BCRP in Trophoblast Cells Impairs the Placental Barrier to Bile Acids During Maternal Cholestasis." *Toxicology and Applied Pharmacology* 277: 77–85.

Cardoso-Moreira, M., J. Halbert, H. Kaessmann et al. 2019. "Gene Expression Across Mammalian Organ Development." *Nature* 571: 505–509.

Davson, H., and M. B. Segal. 1996. *Physiology of the CSF and Blood-Brain Barriers*. Boca Raton, FL: CRC Press.

Dazert, P., K. Meissner, S. Vogelgesang, et al. 2003. "Expression and Localization of the Multidrug Resistance Protein 5 (MRP5/ABCC5), a Cellular Export Pump for Cyclic Nucleotides, in Human Heart." *American Journal of Clinical Pathology* 163: 1567–1577.

Dean, M., and M. Dean. 2002. *The Human ATP-Binding Cassette (ABC) Transporter Superfamily*. Bethesda, MD: National Center for Biotechnology Information (US).

Dey, A., J. E. Jones, and D. W. Nebert. 1999. "Tissue- and Cell Type-specific Expression of Cytochrome P450 1A1 and Cytochrome P450 1A2 mRNA in the Mouse Localized in Situ Hybridization." *Biochemical Pharmacology* 58: 525–537.

Dreier, J. W., A.-M. N. Andersen, and G. Berg-Beckhoff. 2014. "Systematic Review and Meta-Analyses: Fever in Pregnancy and Health Impacts in the Offspring." *Pediatrics* 133: e674–e688.

Dziegielewska, K. M., C. A. N. Evans, P. C. W. Lai, et al. 1981. "Proteins in Cerebrospinal Fluid and Plasma of Fetal Rats During Development." *Developmental Biology* 83: 193–200.

Dziegielewska, K. M., M. Habgood, S. E. Jones, M. Reader, and N. R. Saunders. 1989. "Proteins in Cerebrospinal Fluid and Plasma of Postnatal *Monodelphis domestica* (Grey Short-Tailed Oposum)." *Comparative Biochemistry and Physiology* 92: 569–576.

Eckford, P. D. W., and F. J. Sharom. 2006. "P-glycoprotein (ABCB1) Interacts Directly With Lipid-based Anti-Cancer Drugs and Platelet-Activating factors." *Biochemistry and Cell Biology* 84: 1022–1033.

Ejiri, N., K.-I. Katayama, H. Nakayama, and K. Doi. 2001. "Expression of Cytochrome P450 (CYP) Isozymes in Rat Placenta Through Pregnancy." *Experimental and Toxicologic Pathology* 53: 387–391.

Ek, C. J., K. M. Dziegielewska, H. Stolp, and N. R. Saunders. 2006. "Functional Effectiveness of the Blood-Brain Barrier to Small Water Soluble Molecules in Developing and Adult Opossum (*Monodelphis domestica*)." *Journal of Comparative Neurology* 496: 13–26.

Ek, C. J., M. D. Habgood, K. M. Dziegielewska, and N. R. Saunders. 2003. "Structural Characteristics and Barrier Properties of the Choroid Plexuses in Developing Brain of the Opossum (*Monodelphis domestica*)." *Journal of Comparative Neurology* 460: 451–464.

Ferrada, E., and G. Superti-Furga. 2022. "A Structure and Evolutionary-Based Classification of Solute Carriers." *iScience* 25: 105096.

Frankenberg, S. R., F. R. O. de Barros, J. Rossant, and M. B. Renfree. 2016. "The Mammalian Blastocyst." *WIREs Developmental Biology* 5: 210–232.

Ghosh, C., J. Gonzalez-Martinez, M. Hossain, et al. 2010. "Pattern of P450 Expression at the Human Blood–Brain Barrier: Roles of Epileptic Condition and Laminar Flow." *Epilepsia* 51: 1408–1417.

Ghosh, C., V. Puvenna, J. Gonzalez-Martinez, D. Janigro, and N. Marchi. 2011. "Blood-Brain Barrier P450 Enzymes and Multidrug Transporters in Drug Resistance: A Synergistic Role in Neurological Diseases." *Current Drug Metabolism* 12: 742–749.

Gonzalez, F. J. 1998. "The Study of Xenobiotic-Metabolizing Enzymes and Their Role in Toxicity In Vivo Using Targeted Gene Disruption." *Toxicology Letters* 102–103: 161–166.

Gonzalez, F. J., and D. W. Nebert. 1990. "Evolution of the P450 Gene Superfamily: Animal-Plant 'Warfare', Molecular Drive and Human Genetic Differences in Drug Oxidation." *Trends in Genetics* 6: 182–186.

Greenbaum, D., C. Colangelo, K. Williams, and M. Gerstein. 2003. "Comparing Protein Abundance and mRNA Expression Levels on a Genomic Scale." *Genome Biology* 4: 117.

Habgood, M. D., G. W. Knott, K. M. Dziegielewska, and N. R. Saunders. 1993. "The Nature of the Decrease in Blood-Cerebrospinal Fluid Barrier Exchange During Postnatal Brain Development in the Rat." *The Journal of Physiology* 468: 73–83.

Habgood, M. D., J. E. Sedgwick, K. M. Dziegielewska, and N. R. Saunders. 1992. "A Developmentally Regulated Blood-Cerebrospinal Fluid Transfer Mechanism for Albumin in Immature Rats." *The Journal of Physiology* 456: 181–192.

Hediger, M. A., B. Clémençon, R. E. Burrier, and E. A. Bruford. 2013. "The ABCs of Membrane Transporters in Health and Disease (SLC Series): Introduction." *Molecular Aspects of Medicine* 34: 95–107.

Housman, G., S. Byler, S. Heerboth, et al. 2014. "Drug Resistance in Cancer: An Overview." *Cancers* 6: 1769–1792.

Huang, Y., F. Qiu, M. Habgood, S. Nie, K. Dziegielewska, and N. Saunders. 2023. "Entry of the Antipsychotic Drug, Olanzapine, Into the Developing Rat Brain in Mono- and Combination Therapies." *F1000Research* 11: 1417. https://doi.org/10.12688/f1000research.128074.2.

Jalili, V., E. Afgan, Q. Gu, et al. 2020. "The Galaxy Platform for Accessible, Reproducible and Collaborative Biomedical Analyses: 2020 Update." *Nucleic Acids Research* 48: W395–W402.

Kinsella, R. J., A. Kähäri, S. Haider, et al. 2011. "Ensembl BioMarts: A Hub for Data Retrieval Across Taxonomic Space." *Database* 2011: bar030.

Koehn, L., M. Habgood, Y. Huang, K. Dziegielewska, and N. Saunders. 2019. "Determinants of Drug Entry Into the Developing Brain." *F1000Research* 8: 1372.

Koehn, L. M., Y. Huang, M. D. Habgood, et al. 2020. "Effects of Paracetamol (Acetaminophen) on Gene Expression and Permeability Properties of the Rat Placenta and Fetal Brain." *F1000Research* 9: 573.

Koehn, L. M., Y. Huang, M. D. Habgood, et al. 2021. "Efflux Transporters in Rat Placenta and Developing Brain: Transcriptomic and Functional Response to Paracetamol." *Scientific Reports* 11: 19878.

Linton, K. J. 2007. "Structure and Function of ABC Transporters." *Physiology* 22: 122–130.

Liu, Y., A. Beyer, and R. Aebersold. 2016. "On the Dependency of Cellular Protein Levels on mRNA Abundance." *Cell* 165: 535–550.

Löscher, W. 2007. "Drug Transporters in the Epileptic Brain." *Epilepsia* 48: 8–13.

LoVerso, P. R., and F. Cui. 2015. "A Computational Pipeline for Cross-Species Analysis of RNA-seq Data Using R and Bioconductor." *Bioinformatics and Biology Insights* 9: 165–174.

Mao, Q., and X. Chen. 2022. "An Update on Placental Drug Transport and Its Relevance to Fetal Drug Exposure." *Medical Review* 2: 501–511.

Mazaleuskaya, L. L., K. Sangkuhl, C. F. Thorn, G. A. FitzGerald, R. B. Altman, and T. E. Klein. 2015. "PharmGKB Summary: Pathways of Acetaminophen Metabolism at the Therapeutic Versus Toxic Doses." *Pharmacogenetics and Genomics* 25: 416–426.

Meyer zu Schwabedissen, H. E. U., M. Grube, B. Heydrich, et al. 2005. "Expression, Localization, and Function of MRP5 (ABCC5), a Transporter for Cyclic Nucleotides, in Human Placenta and Cultured Human Trophoblasts: Effects of Gestational Age and Cellular Differentiation." *American Journal of Pathology* 166: 39–48.

Mudunuri, U., A. Che, M. Yi, and R. M. Stephens. 2009. "bioDBnet: The Biological Database Network." *Bioinformatics* 25: 555–556.

Povey, S., R. Lovering, E. Bruford, M. Wright, M. Lush, and H. Wain. 2001. "The HUGO Gene Nomenclature Committee (HGNC)." *Human Genetics* 109: 678–680.

Rask-Andersen, M., S. Masuram, R. Fredriksson, and H. B. Schiöth. 2013. "Solute Carriers as Drug Targets: Current Use, Clinical Trials and Prospective." *Molecular Aspects of Medicine* 34: 702–710.

Rees, D. C., E. Johnson, and O. Lewinson. 2009. "ABC Transporters: The Power to Change." *Nature Reviews Molecular Cell Biology* 10: 218–227.

Safran, M., N. Rosen, M. Twik, et al. 2021. "The GeneCards Suite." In *Practical Guide to Life Science Databases*, edited by I. Abugessaisa and T. Kasukawa, 27–56. Singapore: Springer Nature. https://doi.org/10.1007/978-981-16-5812-9_2.

Saunders, N. R., E. Adam, M. Reader, and K. Møllgård. 1989. "*Monodelphis domestica* (Grey Short-Tailed Opossum): An Accessible Model for Studies of Early Neocortical Development." *Anatomy and Embryology* 180: 227–236.

Saunders, N. R., K. M. Dziegielewska, R. M. Fame, M. K. Lehtinen, and S. A. Liddelow. 2023. "The Choroid Plexus: A Missing Link in Our Understanding of Brain Development and Function." *Physiological Reviews* 103: 919–956.

Saunders, N. R., K. M. Dziegielewska, K. Møllgård, and M. D. Habgood. 2018. "Physiology and Molecular Biology of Barrier Mechanisms in the Fetal and Neonatal Brain: Barrier Mechanisms in the Fetal and Neonatal Brain." *The Journal of Physiology* 596: 5723–5756.

Saunders, N. R., K. M. Dziegielewska, K. Møllgård, and M. D. Habgood. 2019. "Recent Developments in Understanding Barrier Mechanisms in the Developing Brain: Drugs and Drug Transporters in Pregnancy, Susceptibility or Protection in the Fetal Brain?" *Annual Review of Pharmacology and Toxicology* 59: 487–505.

Sedláková, I., J. Laco, K. Caltová, et al. 2015. "Clinical Significance of the Resistance Proteins LRP, Pgp, MRP1, MRP3, and MRP5 in Epithelial Ovarian Cancer." *International Journal of Gynecological Cancer* 25: 236–243.

Smith, K. K. 2001. "Early Development of the Neural Plate, Neural Crest and Facial Region of Marsupials." *Journal of Anatomy* 199: 121–131.

Stein, W. D., and T. Litman. 2014. *Channels, Carriers, and Pumps: An Introduction to Membrane Transport*. Amsterdam, the Netherlands: Elsevier.

Strazielle, N., and J.-F. Ghersi-Egea. 1999. "Demonstration of a Coupled Metabolism–Efflux Process at the Choroid Plexus as a Mechanism of Brain Protection Toward Xenobiotics." *Journal of Neuroscience* 19: 6275–6289.

Syme, M. R., J. W. Paxton, and J. A. Keelan. 2004. "Drug Transfer and Metabolism by the Human Placenta." *Clinical Pharmacokinetics* 43: 487–514.

Szklarczyk, D., A. L. Gable, D. Lyon, et al. 2019. "STRING v11: Protein–Protein Association Networks With Increased Coverage, Supporting Functional Discovery in Genome-Wide Experimental Datasets." *Nucleic Acids Research* 47: D607–D613.

Tyndale-Biscoe, H. 2005. *Life of Marsupials*. Clayton, Australia: CSIRO Publishing. https://ebooks.publish.csiro.au/content/9780643092204/9780643092204.

Vandeberg, J. L., and S. Williams-Blangero. 2010. "The Laboratory Opossum." In *The UFAW Handbook on the Care and Management of Laboratory and Other Research Animals*, 246–261. Hoboken, NJ: John Wiley & Sons, Ltd. https://onlinelibrary.wiley.com/doi/abs/10.1002/9781444318777.ch19.

Vasiliou, V., K. Vasiliou, and D. W. Nebert. 2009. "Human ATP-Binding Cassette (ABC) Transporter Family." *Human Genomics* 3: 281–290.

Wheaton, B. J., J. K. Callaway, C. J. Ek, K. M. Dziegielewska, and N. R. Saunders. 2011. "Spontaneous Development of Full Weight-Supported Stepping After Complete Spinal Cord Transection in the Neonatal Opossum, *Monodelphis domestica*." *PLoS ONE* 6: e26826.

Wheaton, B. J., N. M. Noor, S. C. Whish, et al. 2013. "Weight-Bearing Locomotion in the Developing Opossum, *Monodelphis domestica* Following Spinal Transection: Remodeling of Neuronal Circuits Caudal to Lesion." *PLoS ONE* 8: e71181.

Wheaton, B. J., J. Sena, A. Sundararajan, P. Umale, F. Schilkey, and R. D. Miller. 2020. "Identification of Regenerative Processes in Neonatal Spinal Cord Injury in the Opossum (*Monodelphis domestica*): A Transcriptomic Study." *Journal of Comparative Neurology* 529: 969–986.

Wilcox, S. M., H. Arora, L. Munro, et al. 2017. "The Role of the Innate Immune Response Regulatory Gene ABCF1 in Mammalian Embryogenesis and Development." *PLoS ONE* 12: e0175918.

Workman, A. D., C. J. Charvet, B. Clancy, R. B. Darlington, and B. L. Finlay. 2013. "Modeling Transformations of Neurodevelopmental Sequences Across Mammalian Species." *Journal of Neuroscience* 33: 7368–7383.

World Health Organization. 2012. "Persisting Pain in Children Package: WHO Guidelines on the Pharmacological Treatment of Persisting Pain in Children With Medical Illnesses." [*Conjunto de documentos sobre el dolor persistente en niños: directrices de la OMS sobre el tratamiento farmacológico del dolor persistente en niños con enfermedades médicas*]. World Health Organization. Last modified 30 October 2012. https://apps.who.int/iris/handle/10665/44540.

Zamek-Gliszczynski, M. J., K. A. Hoffmaster, X. Tian, et al. 2005. "Multiple Mechanisms Are Involved in the Biliary Excretion of Acetaminophen Sulfate in the Rat: Role of Mrp2 and Bcrp1." *Drug Metabolism and Disposition* 33: 1158–1165.

Zamek-Gliszczynski, M. J., K. Nezasa, X. Tian, et al. 2006. "Evaluation of the Role of Multidrug Resistance-Associated Protein (Mrp) 3 and Mrp4 in Hepatic Basolateral Excretion of Sulfate and Glucuronide Metabolites of Acetaminophen, 4-Methylumbelliferone, and Harmol in *Abcc3*–/– and *Abcc4*–/– Mice." *Journal of Pharmacology and Experimental Therapeutics* 319: 1485–1491.

Zhang, S., T. R. H. Regnault, P. L. Barker, et al. 2015. "Placental Adaptations in Growth Restriction." *Nutrients* 7: 360–389.

Supporting Information

Additional supporting information can be found online in the Supporting Information section.